Peer Review File

Manuscript Title: Growth of diamond in liquid metal at 1 atmosphere pressure

Reviewer Comments & Author Rebuttals

Reviewer Reports on the Initial Version:

Referees' comments:

Referee #1 (Remarks to the Author):

Making diamond at low pressure is a remarkable achievement because graphite is thermodynamically stable at low pressure. We know that, in principle, with the right kinetic conditions one can prepare a metastable phase. But there is a big difference between knowing that this is possible and knowing how to do it. The authors have managed to find a way.

There is a lot of work on the catalytic decomposition of methane by molten metal alloys that is very similar to the work presented in this paper. However, all such attempts produced graphitic carbon. There is something very unusual about the melt used in this work.

I recommend publication after the authors consider my recommendations.

1. The introduction discusses the high pressure, high temperature process for diamond making. However, it says nothing about CVD and plasma methods which are low pressure and low temperature. They should be briefly mentioned and perhaps compared to the present work.

2. There is no discussion of the quality of the diamond. What is it good for: as a semiconductor, for hardening tools, for jewelry? A sentence or two on this would be helpful.

3. EPR measurements for detecting and characterizing the impurities or defects in the diamond would be helpful. They should be performed if the authors have access to an EPR facility.

4. All papers on methane pyrolysis catalyzed by a variety of molten metal alloys have found that the carbon is contaminated by the catalyst. The contaminants could not be removed by acids, which means that they were chemically bonded to carbon or encapsulated in it. I expect that the diamond would be similarly contaminated. The manuscript should address this.

5. Under the conditions used in this paper the methane decomposes and makes carbon and hydrogen. Why is extra hydrogen added?

6. Work on pyrolysis has shown that catalytic performance depends on the “solvent”. Ga, In, Sn, Pb, Bi have been used. The present work would be strengthened by examining some of these solvents. This would take a month or two of experimental work.

7. I think that the process is made unnecessarily complicated by using a graphite crucible which

apparently is a source of carbon along with methane. It would be helpful to repeat some of these experiments with a quartz crucible.

8. The Upham paper (cited in the manuscript) showed that in the catalytic decomposition of methane by molten metal alloys the carbon produced by reaction dissolves in the melt. It would be good to know if this is the case here. This could be a carbon source for diamond growth.

Minor points:
Lines 33, 34: “synthesize diamonds from melted iron sulfide”. This is an alchemist’s dream. The authors probably meant “synthesize diamonds by using a molten iron sulfide catalyst”.
Line 44: replace “The new growth diamond” with “The diamond grown in this way”.
Line 64: “It is reported that liquid metal acts as catalyst to dissolve carbon”. I would prefer “molten metal acts as a solvent that dissolves carbon”
Lines 74-76: A statement was made that liquid metals are good catalysts because they have an abundance of electrons and ions. Solid metals have the same abundance of electrons and ions as the liquid ones. Please remove those lines.

Referee #2 (Remarks to the Author):

Natural diamonds obtained from the earth is thought to grow in a high pressure and high temperature (HPHT) condition, while synthetic diamond can be produced by both HPHT methods (with or without using metal catalyst) and chemical vapor deposition (CVD) processes at atmospheric pressure or lower pressure. In this work, the authors present a new process for the synthesis of diamond in liquid metal with Ni, Fe and Si addition at 1 atmosphere pressure. The study carried out here is systematic, different parameters for diamond growth have been examined and the products are also well characterized. In fact, the synthesis of diamond at ambient pressure or pressure lower than 1 atmosphere is not novel since CVD methods already realize this goal and it is well developed now. The new method for diamond growth presented here by using liquid metal sounds interesting which may present new insight on the diamond growth mechanism but the underlying mechanisms are far from being understood, which however, is important for this work and needs to be uncovered. Besides this, there are also some issues need to be addressed.

1. For the diamond growth with CVD process, carbon precursor, for example, CH_4/H_2, is decomposed and then act as carbon source for diamond crystals/films formation. In this case, either a diamond seed or a substrate (such as Si, Mo and Iridium modified substrate) is used for diamond growth. There are similarities between CVD and the process reported here, such as high temperature condition, and the same carbon source. Thus, the CVD for diamond synthesis should also be mentioned in the background introduction and even compared with their result discussion, such as growth mechanism.
For the diamond growth mechanism, most discussion is based on speculation. I strongly suggest an atomic level understanding of the diamond formation mechanism by theoretical simulation, to show

how the graphite crucible (but not other carbon source) and the decomposed CH4 transform into diamond in liquid metal. This is very important and would be very helpful to improve the work.

2. As the authors stated, Raman spectra of the samples show the presence of diamond together with graphitic carbon. Does this mean graphitic carbon was firstly formed and then was catalyzed into diamond? For example, it has been reported that metal catalysts (or some metal atoms) diffuse into "graphite structure" and catalyze the diamond growth at high temperature, see recent literatures, such as PNAS 119(16): e2201451119 (2022).

3. Size distributions of the diamond crystals from each typical experiment runs should be statistically counted and compared. Are these Raman bands actually characteristic for nanosized diamonds? (see figure2 and figure S24)

4. It is stated that Si is critical for the growth of diamonds. Did the authors see where the Si went to after the diamond growth?

5. It is very strange that the graphite crucible after annealing shows a much more intense D band than that of the as-received one. Are there any structural changes or reaction due to impurities? Note that the graphite crucible also supply carbon source for the diamond growth. This may affect the diamond formation and should be carefully explored and explained.

6. Is the laser of the pyrometer always on during diamond growth? This may also contribute to the diamond synthesis (for example, CH4 decomposition).

Referee #3 (Remarks to the Author):

The manuscript by Gong et al., entitled "Growth of diamond in liquid metal at 1 atmosphere pressure" presents a novel method for growing polycrystalline diamond films using liquid metal at 1 atmospheric pressure and moderate temperatures (1175oC), in the presence of CH4 and H2 gases. The authors assert that polycrystalline diamond films can be successfully grown at the bottom of a graphite crucible in contact with a liquid metal composed of gallium, iron, nickel, and silicon. They propose that diamond growth is facilitated by the catalytic reaction of liquid metals with carbon sources from CH4. The authors employ various characterization techniques such as HR-TEM, EELS, EDS, XPS, and Raman spectroscopy to confirm the phase-pure nature of the diamonds, albeit with Si-V centers.

This manuscript presents a significant breakthrough in diamond growth, challenging prior assumptions regarding the need for high pressures and temperatures in a liquid phase where diamond is the stable phase. The experimental results are convincing and well-documented. However, reviewer feel that few points addressed below need to be addressed before publication.

Comparative Study without Liquid Metal:
Given the similarity in growth conditions between this approach and the hot filament chemical vapor deposition (CVD) process, it is crucial to conduct experiments without liquid metal to confirm

whether diamond growth occurs solely due to the CH4 and H2 gas mixture and the elevated temperature. This would provide valuable insights into the necessity of liquid metal in the process.

Lack of Theoretical Support:
The manuscript lacks theoretical simulations to support the proposed diamond growth mechanism, particularly diffusion of carbon species at the liquid metal-surface interface. While the experimental evidence is clear, theoretical simulations would add depth to the understanding of the process and help establish a more robust mechanism. However, it is understood that this is not trivial and would need more time/work and it may delay this important result, so this is optional.

Role of Silicon:
The manuscript mentions that no diamond growth was observed in the absence of silicon. This finding raises questions about the precise role of silicon in the diamond growth process, which the manuscript does not adequately address. It is essential to explore the mechanism through which silicon influences diamond nucleation and growth.

In summary, the manuscript presents a groundbreaking result in diamond growth at moderate temperatures and at atmospheric pressure using liquid metal. However, to strengthen the scientific rigor of this work, it is recommended to address the points raised above. Once these issues are resolved, this research could significantly contribute to our understanding of diamond growth processes and have broad applications in material science and industry.

Author Rebuttals to Initial Comments:

Response to Reviewers' Comments

RESPONSES ON TWO TOPICS TO ALL REVIEWERS. We reply on two topics for all reviewers, through page R5, as these were common to all 3 reviewers. We then respond to all other individual reviewer remarks (Reviewer 1, then 2, then 3).

1. Is there a difference between our growth method and conventional CVD growth methods, including the mechanism of diamond nucleation and growth by our new approach with liquid metal, and the significance and potential significance of our approach relative to established CVD methods.

The growth of diamonds by low pressure CVD processes can be generally classified into four kinds (based on how the reactants were activated): plasma-assisted CVD, thermally assisted (or "hot-filament") CVD, reactive vapor deposition (for example, combustion methods), and various combinations of these (*Science* 247, 688 (1990); *MRS Bulletin* 23, 22 (1998); *Diamond & Related Materials* 20, 1287 (2011)). Diamonds can be grown on various solid substrate surfaces (that are heated in the range 600-1100 °C) either with or without diamond seeds. A hydrocarbon (usually methane) diluted with hydrogen (to typically 0.1-3 vol% but sometimes higher) is used as a carbon source, and the synthesis is typically done at a pressure less than 1 atm (Liu H, Dandy D S (1996). *Diamond chemical vapor deposition: nucleation and early growth stages*. Elsevier).

A key to the success in growth of diamonds by CVD is the presence of atomic hydrogen in the gas phase, and atomic hydrogen (atomic H) is due to the high energy densities from the various kinds of activation techniques, e.g., plasma, hot filament, and combustion. The relative gasification rates of diamond and graphite are known to differ by orders of magnitude, and atomic H etches graphitic carbon at much higher rates (whereas diamond forms relatively stable C-H bonds on its surfaces so that diamond growth progresses while any graphitic carbon is continuously removed), hence the growth of (metastable) diamond is kinetically favored while that of graphite is hindered by its constant removal. It was also reported that atomic H passivates 'dangling' bonds on the diamond surface and thereby prevents the reconstruction

and graphitization of diamond surfaces to enable further growth of diamond-on-diamond surfaces (*Science* 247, 688 (1990); *Physics-Uspekhi* 58, 134 (2015)).

Our method differs in very significant ways from any of the known CVD methods. For example:

i) Our growths don't involve any high-energy gas-phase activating techniques (plasma, hot-filament, etc.). We 'simply' heat a liquid metal mixture to ~1025 °C (in the region where diamond nucleates and grows).

ii) We find through theoretical modeling that the change in endothermicity for the reaction of methane converting to CH_3 and H radicals, is quite literally "astonishing". (And we note that we have found two more papers in the literature describing very low activation energies for production of H_2(g) from methane by pure gallium—as discussed below.) The bond dissociation energy of methane in the gas phase is ~4.6 eV. However, when methane is adsorbed onto the liquid metal (LM) surface, this reaction energy changes to either a *very small* positive value, or even to negative values—such that CH_4(ads) $\rightleftharpoons$ CH_3(ads) + H(ads), where "ads" means adsorbed on the LM, can be even exothermic per certain configurations we have calculated(!). *The LM activates the methane in this first bond-breaking event, quite extraordinarily.*

   There are also two 'experimental' papers that address the activation of methane by pure gallium that suggest (very) low activation barriers, E_A, that we cite and briefly summarize alongside the section presenting our theoretical modeling. One (*Scientific Reports* 7, 12371 (2017)) presents growth of graphene films at temperatures even close to room temperature; the other is a quite recent study (*Chemical Engineering Journal* 460, 141558 (2023)) of electrostatically levitated droplets of Ga, and separately, of molten In, Sn, Bi, and Cu, that overlaps our growth temperature in their temperature range for their Arrhenius plot from generation of H_2(g) from collisions of methane with the levitated droplets.

iii) Nucleation and growth of diamonds in our LM mixture happens subsurface; CVD diamond growth happens on solid surfaces that are often pre-seeded (but need not always be). Our LM approach does not need any seeding. TEM-EDS of cross section samples, and Time-of-flight secondary ion mass spectrometry (ToF-SIMS) of the solidified liquid

metal (SLM) piece, each show a high [C] (concentration of C) close to the surface that then monotonically falls to a lower [C] at depths such as 100 nm below the surface. The [C] as a function of depth for the early growth stages (5, 10, and 15 min, see more details on Pages R23-27) from the surface of the SLM in a 100 μm x 100 μm SLM region that had been directly adjacent to where a polycrystalline diamond film had grown *differs* from [C] in a 100 μm x 100 μm SLM region nearby (5 mm away) where no diamond grew (no particles and thus no film). We also note: Our measurement of a relatively high [C] in this subsurface region by ToF-SIMS depth-profiling and cross section TEM-EDS is, to the best of our knowledge, the first clear evidence that [C] can be quite high in such a gallium-rich alloy, even though its (thermodynamic) solubility might be either zero or extremely low. (The solubility of C is in pure gallium is perceived to be zero at all temperatures; indeed there is no C-Ga phase diagram published.) And, perhaps most importantly, the subsurface [C] for SLM for the 10 min run is far higher than both the 5 min run and the 15 min run. The 5 and 10 min runs showed no diamond in the central region where diamond films are typically found for, e.g, 150 min runs. But the 15 min run shows diamond particles in the central region. We have clear experimental evidence that diamonds grow subsurface due to a very high [C] being reached at ~10 minutes, and that this extreme supersaturation of C, with Si playing a role, causes nucleation and rapid growth for run times greater than 10 minutes but less than or equal to 15 minutes.

iv) With this new ToF-SIMS data as well as our already described measurement of the temperature gradient present at the bottom of the LM in conditions essentially identical to our growth runs, it is now possible to present a highly plausible model for how diamond nucleates and grows: in the central region when a very high concentration of C atoms is reached, diamond nuclei form that grow and are constantly 'fed' new C by the surrounding, higher temperature regions nearby; Si plays a critical role, per our modeling studies described below, in stabilizing very small carbon clusters in the Ga-Fe-Ni-Si melt (Si-C-C and C-Si-C, and also in stabilizing tetravalently-bonded C in larger clusters. These are the 'pre-nuclei' that can then grow very rapidly once a certain level of supersaturation of C atoms happens—at about 10 minutes.

Thus, the mechanism of growth of diamond in the LM sub-surface region is fundamentally different than any of the CVD methods we are aware of. (We appreciate the question from the reviewers about the possible similarities between our method and CVD growth methods, given our use of methane and hydrogen, that are, as noted, common precursors for CVD growth. We used CH_4 in part because $^{13}CH_4$ is readily available (and affordable!). It will be of interest to explore other hydrocarbon precursors in the future.)

Turning from the completely different mechanism of growth described above, to other differences between this LM approach and, e.g., HPHT or CVD methods, we reiterate the (we think strong) possibility of enabling the large-scale production of diamonds by using a larger surface/interface, by configuring heating elements to achieve a much larger potential growth region, and by distributing carbon to the diamond growth region in some new ways that Ruoff has recently invented and that are now being explored (and that we note are *very early stage*).

And now, we turn to an important topic that is not a part of our work here, but that we forecast could be enabled through our work here: To the best of our knowledge, there is no production of diamond anywhere that is based on the growth of new diamond *on* small diamond particles such as are available in diamond powders of various types. *The most natural way to grow particles is in a liquid solution*. We have a liquid (a highly flexible liquid metal 'platform') that seems likely to enable enlarging small diamond particles by dispersing the diamond particles in appropriate liquid metals. Suppose one has 0.1 μm diameter particles and enlarges them, to, say, 1.0 μm particles (10-fold increase in diameter). This is a 999-fold increase in new diamond. This will be revolutionary! We are aiming to achieve this in liquid metals at low pressure in the (hopefully) near future—an entirely different project in our group that is relatively 'early stage'. We suggest that it will either be us or others that will (likely) achieve this after our paper is published.

2. Our finding and use of EDM-3 Poco Graphite Plate blocking intimate contact between liquid metal and graphite crucible bottom surface to enable growth of diamonds from methane.

First, we note that in our (revised) manuscript we have chosen to emphasize that use of the

EDM-3 Poco Graphite plate almost completely eliminates any other C than from the methane being incorporated into the grown diamonds, as show from our $^{13}CH_4$ studies with the EDM-3 plate in place. Our focus, now, is entirely on the use of this non-contributing interface material EDM-3; *now, the crucible graphite never contacts the LM in the critical growth region* during all of our recent and current experimental runs.

When liquid metal was placed directly contacting the graphite crucible bottom surface and $^{13}CH_4$ was introduced for the growth, the diamonds were grown from the carbon of both $^{13}CH_4$ and the graphite crucible, and the graphite crucible contributes larger amounts of carbon for growth (Fig. 2b). However, the grown diamonds were of 'bad quality' showing an intense Raman G band compared to when there are EDM-3 Poco Graphite plate(s) or an HOPG piece placed at the interface (then it is the methane that dominates, including entirely in some cases, in terms of the source of C for the diamond growth; and the diamonds are of higher quality, and free of graphite such as in diamond films after 150 min runs). This strongly suggests (shows) that methane is a better carbon source than the crucible carbon for the growth of high-quality diamond.

In our (originally) submitted manuscript, we described that we were able to achieve the growth from *only* methane at the interface between the LM and the top layer of a stack of 10 pieces of EDM-3 Poco Graphite plates (stacked from the crucible bottom surface). We now have a new growth done by placing a pyrolytic boron nitride plate (PBN, 1 mm thick; MTI Korea) between liquid metal and the graphite crucible (see details in our response to Comment 7 of Reviewer 1, Pages R21-23). Briefly, by using this kind of non-carbon material, we were able to grow diamond from only methane as the crucible contributes no carbon for the growth (it is 'blocked' by the PBN plate). And the as-grown diamonds were of high quality (showing less graphitic signal than when no PBN or EDM-3 plate is present, i.e., when the LM directly contacts the graphite crucible).

Our revised paper now <u>emphasizes growing diamonds from methane by exclusive use of the EDM-3 plate</u>, as we learned that methane is a better carbon source than the crucible graphite (grows better diamonds) and, also, that efficient growth can be achieved from methane, only.

RESPONSES TO ALL QUESTIONS AND COMMENTS FROM THE 3 REVIEWERS

Referee #1 (Remarks to the Author):

Making diamond at low pressure is a remarkable achievement because graphite is thermodynamically stable at low pressure. We know that, in principle, with the right kinetic conditions one can prepare a metastable phase. But there is a big difference between knowing that this is possible and knowing how to do it. The authors have managed to find a way.

There is a lot of work on the catalytic decomposition of methane by molten metal alloys that is very similar to the work presented in this paper. However, all such attempts produced graphitic carbon. There is something very unusual about the melt used in this work.

I recommend publication after the authors consider my recommendations.

Response:

Thank you for reviewing our paper.

1. The introduction discusses the high pressure, high temperature process for diamond making. However, it says nothing about CVD and plasma methods which are low pressure and low temperature. They should be briefly mentioned and perhaps compared to the present work.

Response:

Thank you for your comment. Please see the 1st section in the RESPONSES ON TWO TOPICS TO ALL REVIEWERS on Pages R1-R4.

We have added descriptions of CVD growth methods in the Introduction.

2. There is no discussion of the quality of the diamond. What is it good for: as a semiconductor, for hardening tools, for jewelry? A sentence or two on this would be helpful.

Response:

Thank you for your comment.

Our as-grown diamond film is of high quality:

i) EELS spectra acquired from 20 randomly selected regions over the diamond region show only one major σ* peak (Fig. 3e), suggesting the whole region is a uniform diamond film.

ii) Plan-view HRTEM images (Fig. S25) and the SAED ring pattern and the associated (calculated) radial intensity profile (Fig. S26) of the as-grown diamond film shows only diamond phase. There were no graphitic structures found between diamond particles.

iii) We did UV Raman mapping of the full width half maximum (FWHM) of the diamond Raman band (at 1332 cm^{-1}) of our as-grown diamond film and an as-purchased polycrystalline CVD-grown diamond piece (5 mm x 5 mm x 0.5 mm, Changsha 3 better Ultra-hard Materials) as shown in Fig. R1. We found that over the 200 μm × 200 μm regions our as-grown diamond film has a more uniform *and* narrower FWHM than the as-purchased one, which shows our as-grown diamond film has higher crystallinity.

iv) Time-of-flight secondary ion mass spectrometry (ToF-SIMS) depth-profiling over a lateral size of 100 μm x 100 μm of our as-grown diamond film showed no Ga, Ni, Fe and Si detected even to 50 nm depth (Fig. R2).

Thus, our as-grown polycrystalline diamond film is of high-quality regarding purity of diamond phase, with grain sizes of ~300 nm. The intense PL peak at 738.5 nm and thus SiV^- color centers in our as-grown diamonds suggest possible use in electronic devices including quantum computing.

Additionally, we suggest our growth of diamonds in liquid metal at moderate temperature and 1 atm pressure opens many possibilities for further studies and for the scaling of this type of growth, and when larger polycrystalline and single crystals are produced in the future (by us or someone else), various applications will be vigorously pursued. And we reiterate the likelihood of large-scale production of 'solution' grown diamond particles described above.

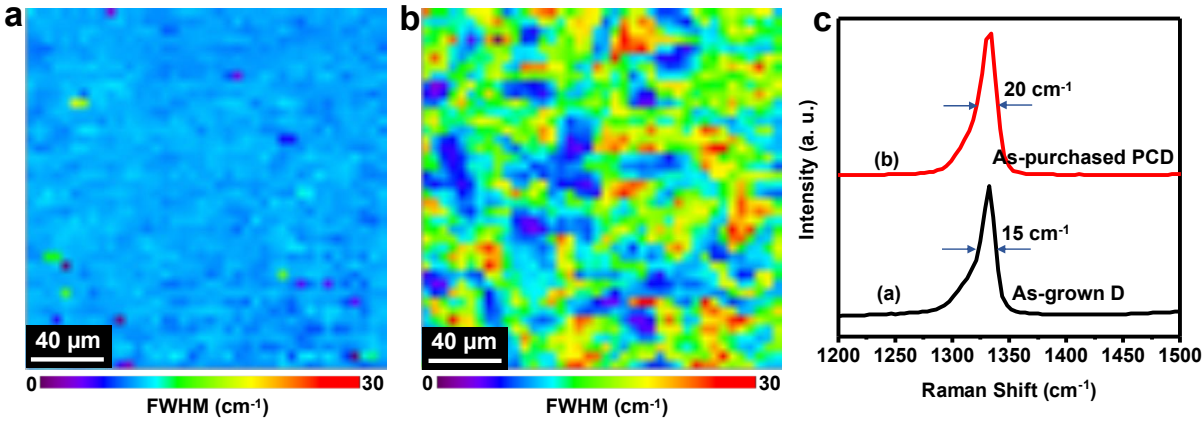

Figure R1. Raman analysis (obtained with 266 nm laser) of as-grown diamond film after transferring onto a 300 nm SiO_2/Si wafer surface and of as-purchased polycrystalline diamond piece. Raman map of FWHM of diamond peak at 1332 cm^{-1} of (a) the as-grown diamond film and (b) the as-purchased diamond substrate. (c) Averaged Raman spectra obtained from the entire mapped regions of (a) and (b).

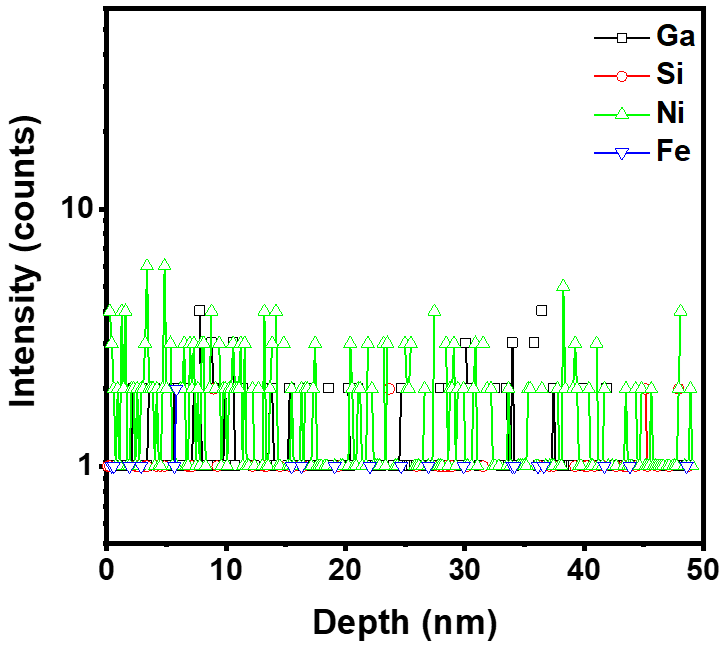

Figure R2. ToF-SIMS depth-profiling (Intensity as function of the depth) obtained on as-grown diamond film.

3. EPR measurements for detecting and characterizing the impurities or defects in the diamond would be helpful. They should be performed if the authors have access to an EPR facility.

Response:

We thank the reviewer for this suggestion. We do not have ready access to an EPR facility.

Thus, we did ToF-SIMS depth-profiling to study any impurities present in our as-grown diamonds as mentioned above (Fig. R2).

4. All papers on methane pyrolysis catalyzed by a variety of molten metal alloys have found that the carbon is contaminated by the catalyst. The contaminants could not be removed by acids, which means that they were chemically bonded to carbon or encapsulated in it. I expect that the diamond would be similarly contaminated. The manuscript should address this.

Response:

Thank you for your comment.

The as-grown diamond film on solidified liquid metal was delaminated by dissolving the metal alloy piece using HCl(aq) solution and then transferred onto a Cu TEM grid with the back side (the side that is interfacing liquid metal during growth) facing up. ToF-SIMS spectra of C, Ga, Si, Ni and Fe were obtained with different sputtering times (to reach a certain depth) to study any contaminants on the *back side* of the as-transferred diamond film. After surface cleaning (5s sputtering), the ToF-SIMS spectra were acquired, with a large intensity of C and weak intensity of Ga and Si observed (Fig. R3a-c). Very weak intensity of Fe that is very likely due to noise, and no signal for Ni (Fig. R3d and e) were found. The intensity of C was constant after 20s (depth of 2 nm), 80s (depth of 8 nm) and until 140s (depth of 14 nm), while the intensities of Ga and Si were dramatically decreased, suggesting that there are only small amounts of Ga and Si contaminants on the as-transferred diamond film back side surface, but none are detectable in the diamond bulk.

To further study the chemical states of Ga and Si, XPS analysis (Ga $2p_{3/2}$ and Si 2p) was done (Fig. R4) on this back side surface, and it showed native oxide, 'organic silicon', and Si-O bonding. We did not observe any signal of Ga-C, suggesting that the native oxide of gallium is likely physically adsorbed on the back side surface of the diamond film. The presence of Si-C bonds is of interest as we find that a small amount of Si is critical for our diamond growths (see details in our response to Comment 1b of Reviewer 2 on Pages 37-46), while SiO_2 is likely formed due to some Si present atop the (backside) of the diamond film.

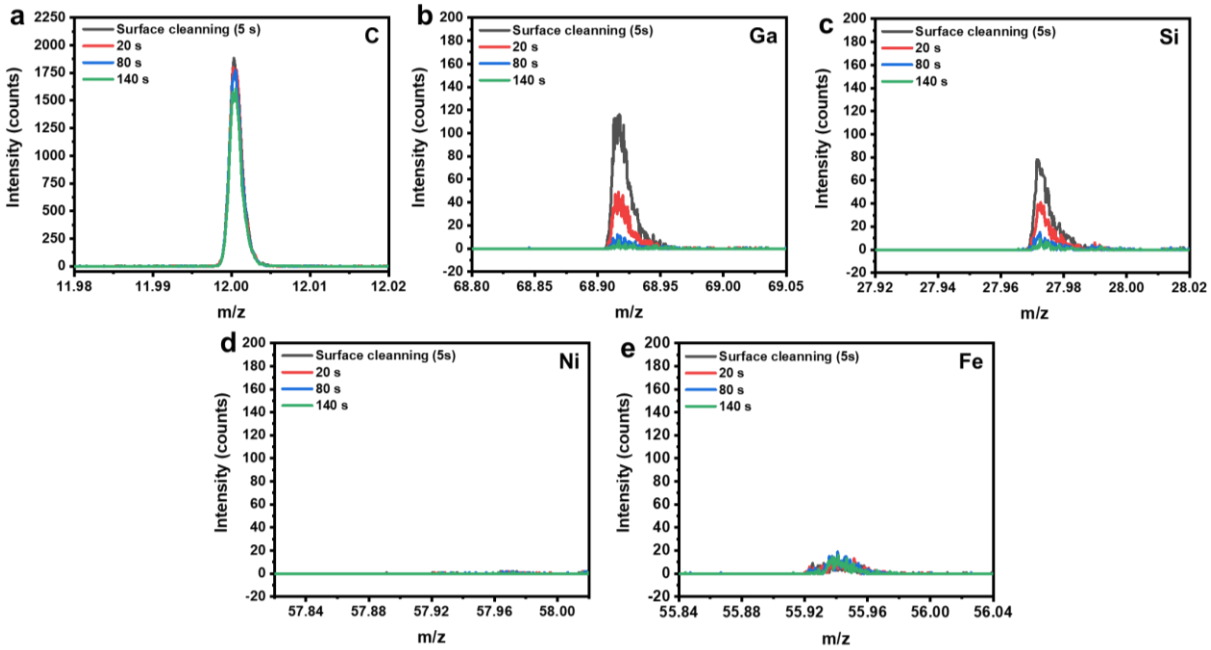

Figure R3. ToF-SIMS spectra of the back side of the as-transferred diamond film (a) C. (b) Ga. (c) Si. (d) Ni. (e) Fe.

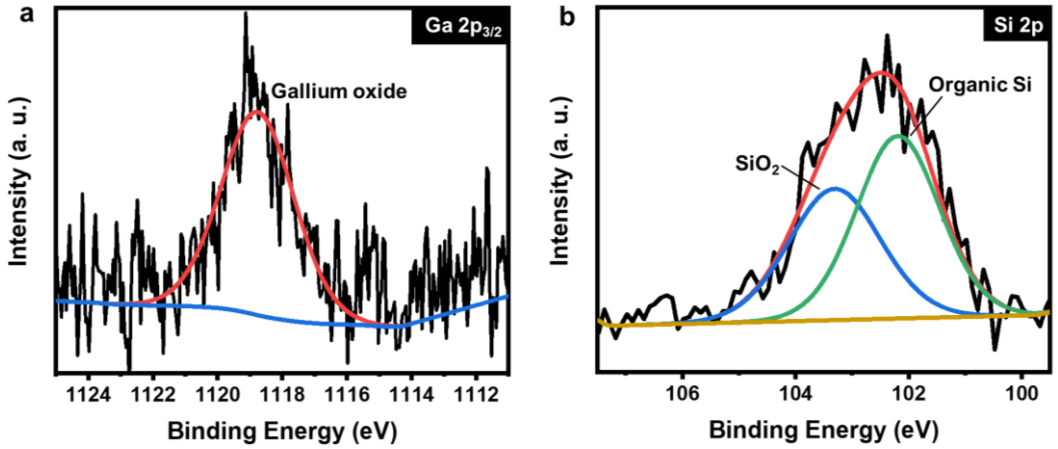

Figure R4. XPS spectra of (a) Ga $2p_{3/2}$ and (b) Si 2p for the back side of as-transferred diamond film.

5. Under the conditions used in this paper the methane decomposes and makes carbon and hydrogen. Why is extra hydrogen added?

Response:

Thank you for asking. We have now done additional experiments to further study the role of H_2 in our diamond growths.

i) We did two growth experiments with no hydrogen present, one with pure methane and the

other with methane diluted in argon. With 1 atm pure CH_4 (with a slight flow through our growth chamber, i.e., not a closed volume) we found thick graphite grown everywhere on the solidified liquid metal piece (Fig. R5a) and no diamond grew. An intense Raman D band observed in the Raman spectrum shows the graphite was defective (Fig. R5b). For CH_4 /Ar of 5/100, we found a very high-quality thick graphite film having no Raman D band (Fig. R5c-d) on all the SLM piece surface, and no diamond grew. These 2 runs suggest that H_2 is needed to grow diamond under our current 'optimal' conditions of the LM mixture of Ga/Fe/Ni/Si (77.75/11/11/0.25 atomic percentages).

ii) Growth experiments with CH_4 /H_2 of 1/100, 2.5/100, 10/100 and 20/100 were done to further study the role of hydrogen in diamond growth. Excepting 1/100 CH_4 /H_2, the 2.5/100, 10/100 and 20/100 gas mixtures all led to diamond formation on the solidified liquid metal surface. For CH_4 /H_2 of 1/100, only amorphous carbon was found on the solidified liquid metal surface (Fig. R6a-b). For CH_4 /H_2 of 2.5/100 diamonds with small crystal size were found. Facets were not clearly exposed, and the quality is 'not good' (Fig. R6c-d). For CH_4 /H_2 of 10/100, the morphology of diamonds is very similar to those obtained in our typical runs (5/100 CH_4 /H_2) (Fig. R6e-f). For CH_4 /H_2 of 20/100, "round ball" shape diamond crystals were grown, with the growth of by-product carbon fibers (Fig. R6g-f, R7).

Our results i) and ii) suggest that appropriate amounts of H_2 (100/2.5 ~ 100/20 of H_2/CH_4 molar ratio; literally volume ratio as we assume ideal gas to obtain mol percentages) is critical for the growth of diamonds. Also: The H_2/CH_4 should not be *larger* than 100/2.5; when it is, diamond does not grow, likely due to insufficient carbon in the source gas for the growth.

We did a growth by replacing H_2 with D_2 and obtained ToF-SIMS spectra from the as-grown diamonds. We note that for the diamonds grown by using CH_4/ H_2, there is no peak at *m/z* of 2 (for H_2^-; that is 2.01565 amu) and 14 (for CH_2^-; that is 14.01565 amu) (Fig. R8a-b). For the diamonds grown using CH_4/D_2, peaks at *m/z* of 2 and 14 were observed (Fig. R8c-d) and assigned to D^- (2.014102 amu) and CD^- (14.014102 amu). The intensity of these two peaks dramatically decreased after sputtering for 140s (reaching a depth of 14 nm), suggesting that D was mainly present on the diamond surfaces, i.e., the diamond surfaces were hydrogenated.

We note that the very weak (but not zero) intensity of the CD^- peak at the depth of 14 nm is very likely suggesting that there is hydrogen (here, deuterium) present at the grain boundaries between diamond grains, since our as-grown diamond film is polycrystalline.

The Raman spectrum (Fig. R9) of the as-grown diamond film by using CH_4/ H_2 in our standard runs shows a peak at 2878 cm^{-1} that we assign as a C-H stretching peak; this peak is redshifted to 2150 cm^{-1} for the diamond film that is grown by using CH_4/D_2, corresponding to the peak frequency for C-D stretching (*Journal of Applied Physics* 75, 1804 (1994); *Physical Review B* 60, R5165 (1999)). Our Raman studies thus suggest that our as-grown diamond surfaces are terminated by hydrogen.

We delaminated (by using a double-side copper tape) the as-grown diamond film from the D_2/CH_4 growth (discussed above) and obtained ToF-SIMS data from the diamond-grown region on the solidified liquid metal (SLM) piece. The data show the ions D^- (2.014102 amu), $^{12}CD^-$ (14.014102 amu), $^{69}GaD^-$ (70.939675 amu), $^{58}NiD^-$ (59.949444 amu) present in the SLM piece, with intensities decreasing from a depth of 10 nm (sputtering for 50s), to depths of 40 nm (sputtering for 200s) and 300 nm (sputtering for 1500s) (Fig. R10a-d). We note that the mass of $^{56}FeD^-$ (57.949037 amu) is very close to $^{58}Ni^-$ (57.935342 amu) and thus we cannot assign its possible presence. It has not been possible to assign the concentration of D as a function of depth, as we do not have a method of correlating the actual [D] to the ion yields mentioned. We show this data to the reviewers as it shows that D is subsurface in the SLM. Its role is perhaps only relevant when the diamond particles grow significantly larger, but we acknowledge that this is a topic for further study in the future.

In summary, our studies to date suggest hydrogen should be introduced to grow diamond by our method. Our as-grown diamond surfaces are hydrogen-terminated.

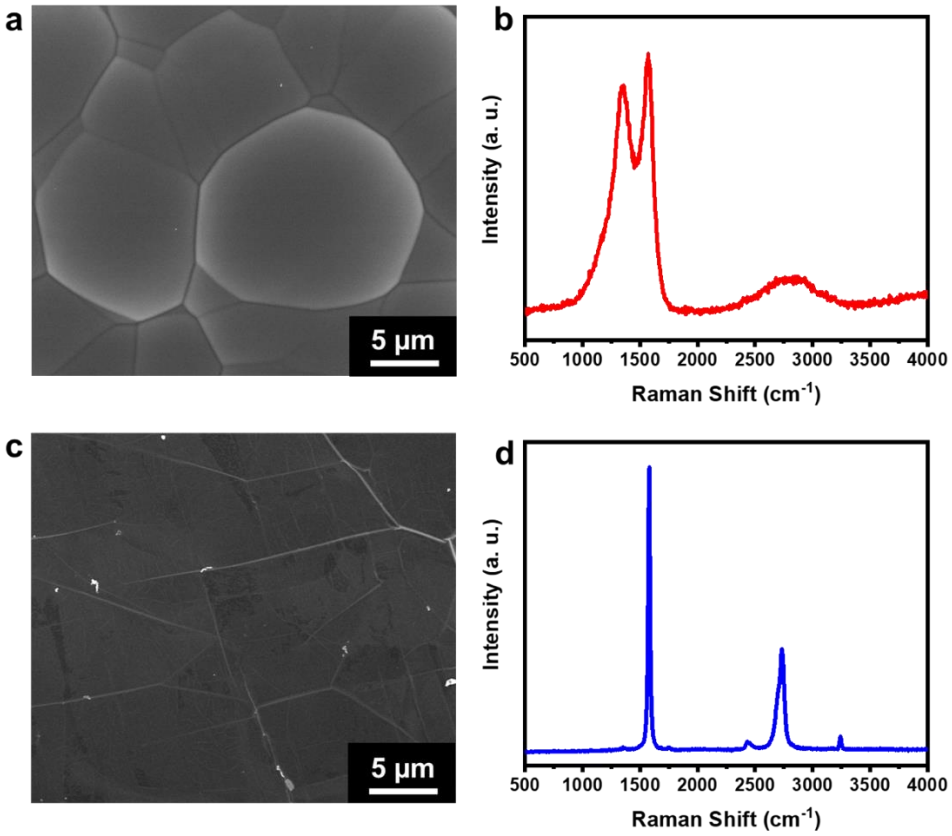

Figure R5. SEM images and Raman spectra of the growths with no H_2 present. (a, b) The growth with only CH_4 present. (c, d) The growth with 5/100 CH_4/Ar. Experiment parameters: 1175 ºC, 760 Torr, 150 min, 0.25 at% Si, 11.00 at% Ni, 11.00 at% Fe, 77.75 at% Ga.

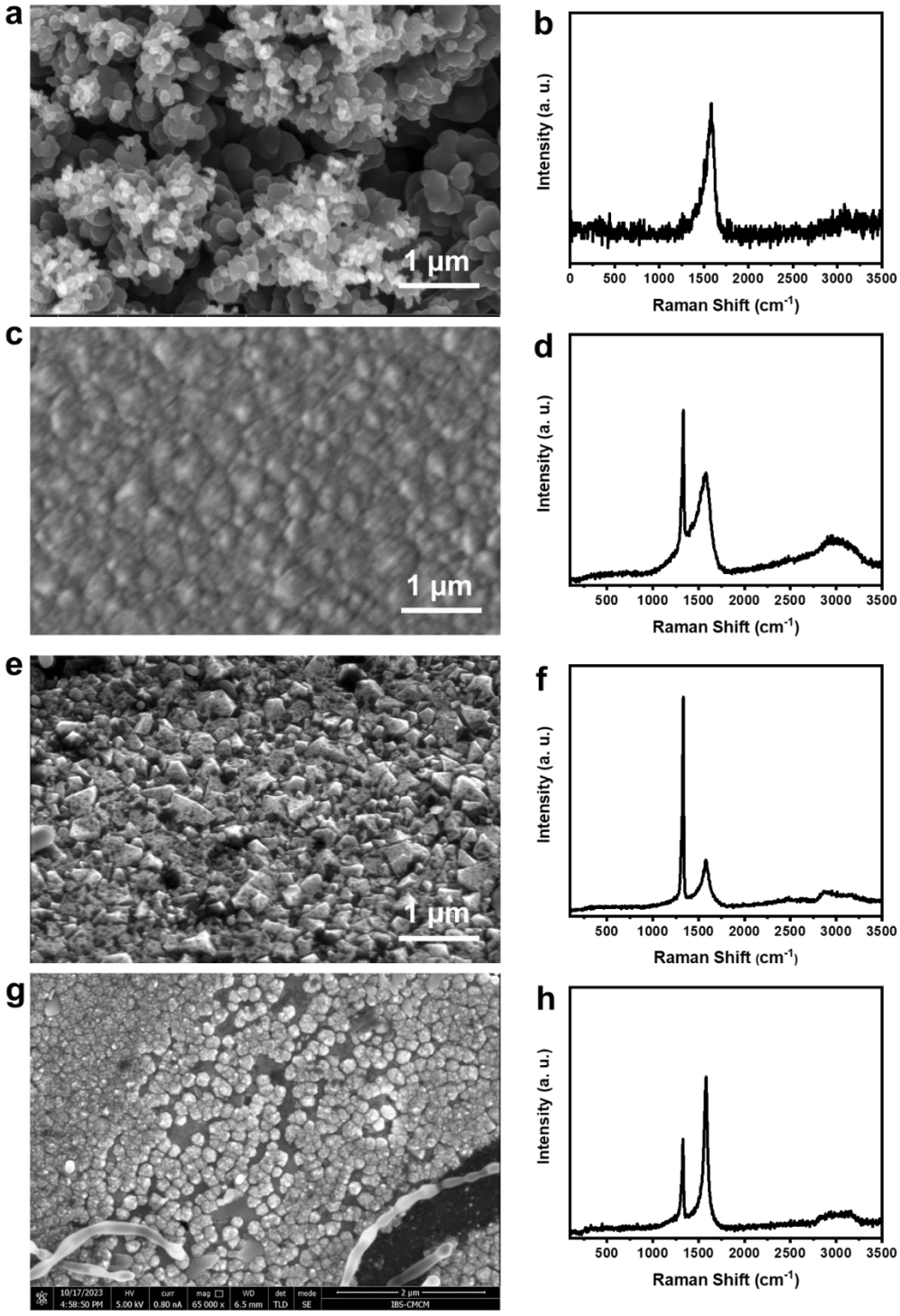

Figure R6. SEM images and Raman spectra of the growths with different ratios of CH_4 /H_2. (a, b) 1/100 CH_4 /H_2. (c, d) 2.5/100 CH_4 /H_2. (e, f) 10/100 CH_4 /H_2. (g, h) 20/100 CH_4 /H_2. Experiment parameters: 1175 ºC, 760 Torr, 150 min; 0.25 at% Si, 11.00 at% Ni, 11.00 at% Fe, 77.75 at% Ga.

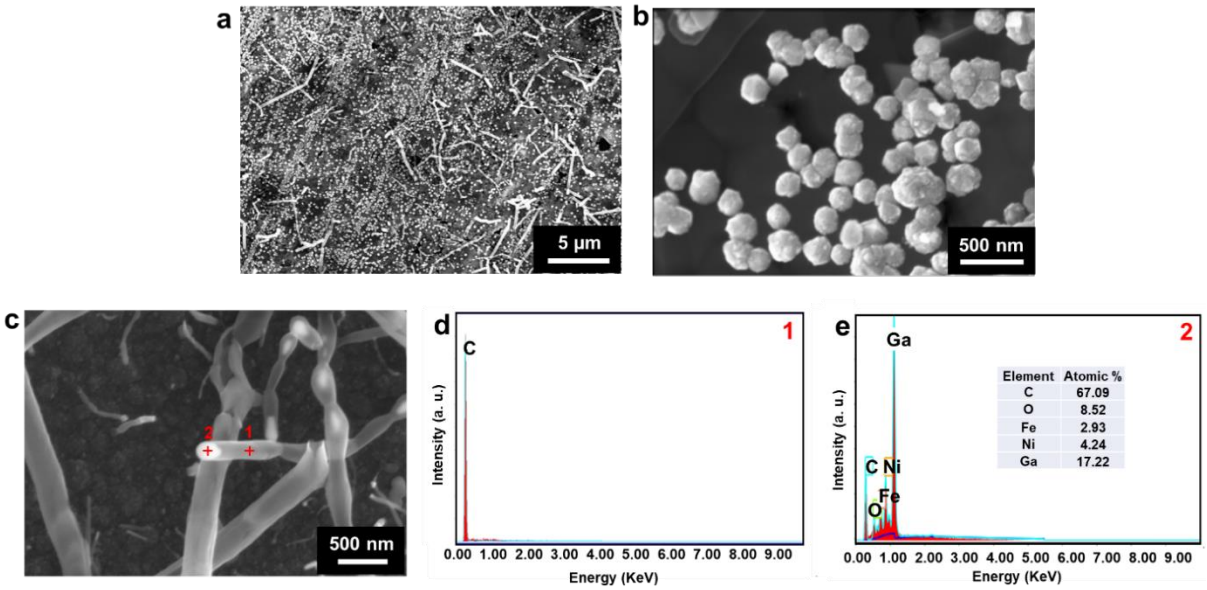

Figure R7. SEM images and EDS analysis of the growth using 20/100 CH_4/H_2. (a) Low magnification SEM image of diamond crystals and carbon fibers grown on metal alloy piece. (b) High magnification SEM image of diamond crystals grown on metal alloy piece. (c) High magnification SEM image of carbon fiber. EDS analysis of regions 1 (d) and 2 (e) of carbon fibers in (c).

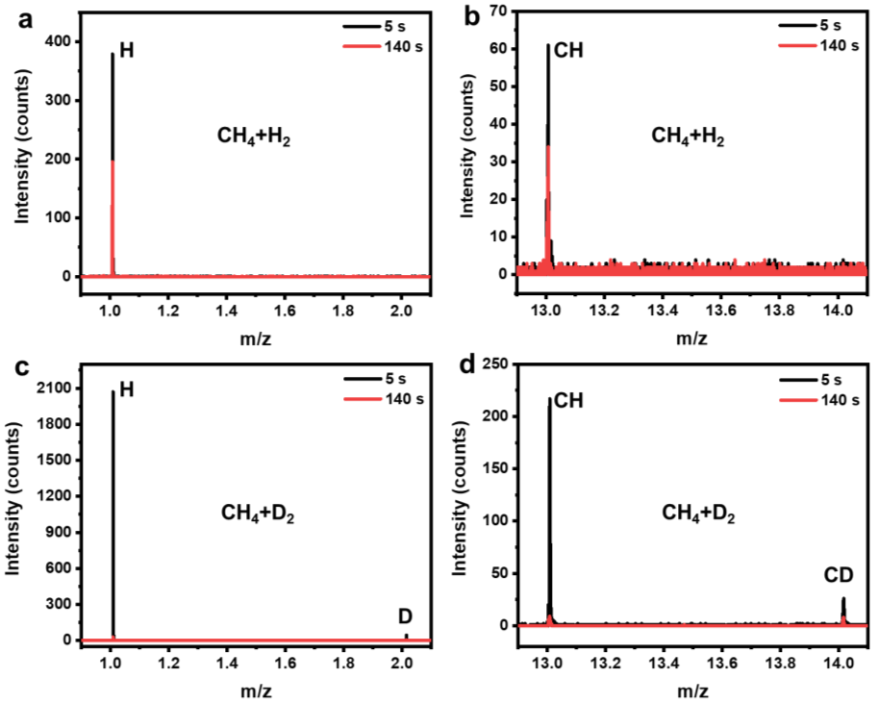

Figure R8. ToF-SIMS surface spectra of the D-labeled as-grown diamond film (solidified liquid metal piece from the run with CH_4/ D_2 (5/100)) compared to a typical run (of CH_4/ H_2 (5/100)). H peak (a) and CH peak (b) of the as-grown diamond film of CH_4/ H_2 after 5s and 140s sputtering. The peaks of H and D (c), and CH and CD (d) of the as-grown diamond film of CH_4/ D_2 after 5s and 140s sputtering.

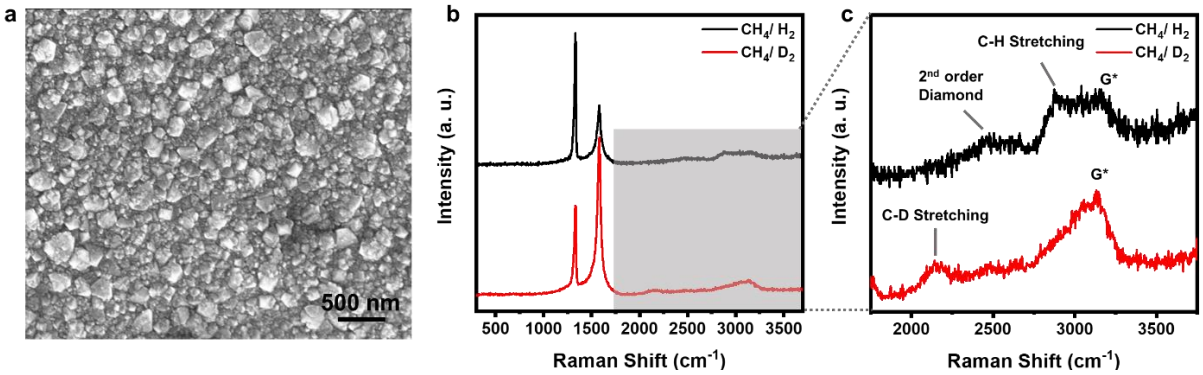

Figure R9. SEM image and UV Raman analysis of the D-labeled as-grown diamond film. (a) SEM image. (b) UV Raman spectra of D-labeled as-grown diamond film compared to the typical one generated by our optimized run with normal methane and hydrogen gases. (c) An expanded view of (b) that shows the typical diamond C-H stretching peak compared to D-labeled diamond.

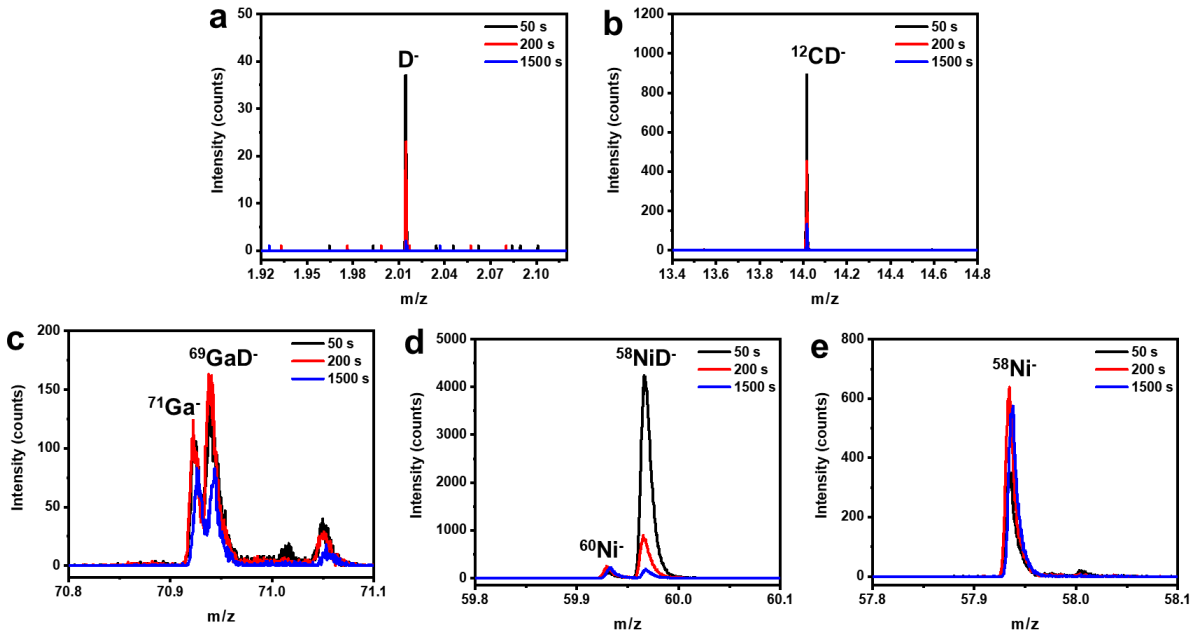

Figure R10. ToF-SIMS surface spectra of the SLM for the CH_4/ D_2 (5/100) run at 50, 200, and 1500 seconds. (a) D^- peaks. (b) $^{12}CD^-$ peaks. (c) $^{71}Ga^-$ and $^{69}GaD^-$ peaks. (d) $^{60}Ni^-$ and $^{58}NiD^-$ peaks. (e) $^{58}Ni^-$ peaks.

6. Work on pyrolysis has shown that catalytic performance depends on the "solvent". Ga, In, Sn, Pb, Bi have been used. The present work would be strengthened by examining some of these solvents. This would take a month or two of experimental work.

Response:

Thank you for your comment. We've now tried other 'solvent metals'.

The binary phase diagrams of Sn, In, Pb and Bi with Ni, and Fe, are shown in Fig. R11. As can be seen all four elements can be mixed well with Ni and Si to form liquid alloy at our experimental temperature (~1025 ºC). However, only Sn and In can form liquid alloys with Fe. Therefore, considering our typical (i.e., optimized) growth with Ga/Ni/Fe/Si, and replacing Ga with other kinds of metals, Sn and In were our first choices. We thus did the experiments by replacing Ga with Sn, and Ga with In, respectively. All the experiments were done at 1175 ºC (temperature of graphite crucible wall read by pyrometer—in short, our standard approach), 760 Torr, with CH_4/H_2 5 sccm/100 sccm, for 150 min.

i) Replacing Ga to Sn: For the growth by using $Sn_{77.75}/Ni_{11}/Fe_{11}/Si_{0.25}$, there was only a small amount of graphitic carbon deposited on the solidified liquid metal surface (Fig. R12a-b). We then tried a 50/50 (atomic ratio) Ga/Sn mixture: defective graphite structures were found to be grown when using $Ga_{38.88}/Sn_{38.87}/Ni_{11}/Fe_{11}/Si_{0.25}$ (Fig. R12c-d), and hexagonal shape graphite islands grew when using $Ga_{38.88}/Sn_{38.87}/Ni_{14.67}/Fe_{7.33}/Si_{0.25}$ (Fig. R12e-f). We note that all 3 mixtures seemed to form homogenous liquid alloys under our growth temperature (by evaluating the solidified liquid metal piece later), and no diamonds grew in these 3 experiments.

ii) Replacing Ga with In: We first tried $In_{77.75}/Ni_{11}/Fe_{11}/Si_{0.25}$, and only defective graphite structures were found on the solidified liquid metal surface (Fig. R13a-b). We then used a 50/50 (atomic ratio) Ga/In mixture instead of using only In. For the mixture of $Ga_{38.88}/In_{38.87}/Ni_{11}/Fe_{11}/Si_{0.25}$, vertical graphite structures were found on the solidified liquid metal surface (Fig. R13c-d). There were no diamonds found in either of these experiments.

However, when using $Ga_{38.88}/In_{38.87}/Ni_{14.67}/Fe_{7.33}/Si_{0.25}$ (a homogenous liquid alloy was formed at the growth temperature), we found a 'transparent but dark' film on the solidified liquid metal surface (adjacent to the EDM-3 Poco graphite sheet piece). This film was delaminated by using a double-side copper tape and transferred onto a 300 nm SiO_2/Si wafer substrate (Fig. R14a-b). This film is a diamond film per UV Raman spectroscopy (Fig. R14d), but the quality of the film (showing a very intense graphite G band) is a bit

worse compared to our typical growth using Ga/Ni/Fe/Si. The facets were also not clear (Fig. R14c).

In summary, a Ga/In (50/50 atomic ratio) can be used to grow diamonds, specifically with $Ga_{38.88}/In_{38.87}/Ni_{14.67}/Fe_{7.33}/Si_{0.25}$, thus by lowering the Fe content and increasing the Ni content. We note that the parameter space is large and perceive that Sn, Pb, or Bi could be used as solvents including when alloyed with other metals, and by growth runs with other than methane. Given our focus on using methane, including because of the ready availability of ^{13}C-labeled methane, other precursors (e.g., acetylene, ethylene, allene, etc.) can be explored in the future, further expanding parameter space. We suggest that our work here will lead to a surge of efforts along these lines by the world-wide community.

As one example of how remarkably different the hydrocarbon precursor can be in terms of reactions involving metals, we note the low temperature (below room temperature!) conversion of acetylene to benzene and also on to further products on the pristine Cu(111) surface (*The Journal of Physical Chemistry B* 109, 10952 (2005)), whereas methane has no reactivity at all at low temperatures on Cu(111) (*The Journal of Physical Chemistry B* 122, 855 (2018)).

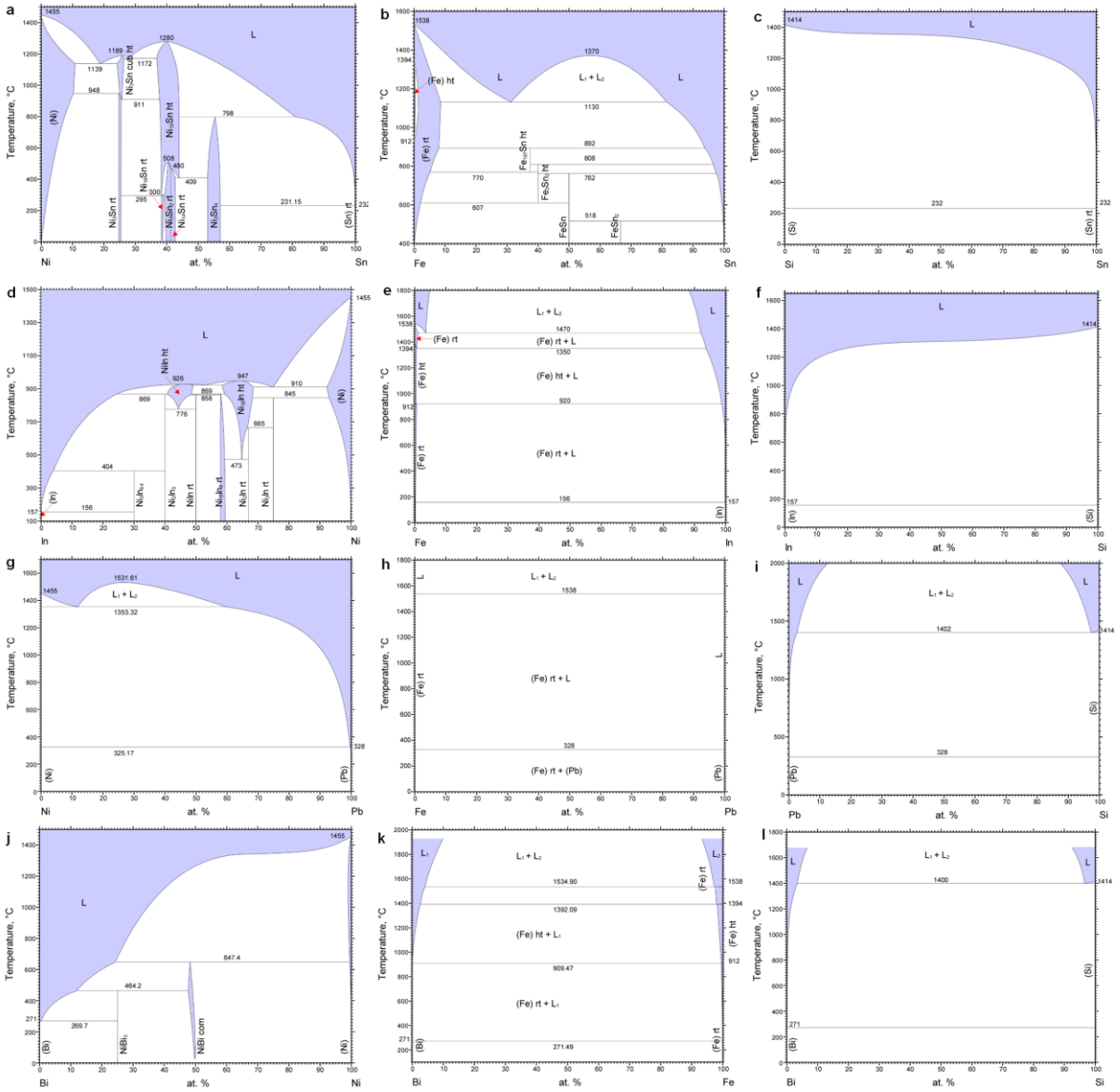

Figure R11. Binary phase diagram of Sn, In, Pb and Bi with Ni and Fe, respectively. (a) Sn/Ni. (b) Sn/Fe. (c) Sn/Si. (d) In/Ni. (e) In/Fe. (f) In/Si. (g) Pb/Ni. (h) Pd/Fe. (i) Pb/Si. (j) Bi/Ni. (k) Bi/Fe. (l) Bi/Si. All phase diagrams are reproduced from the *ASM Alloy Phase Diagram Database*.

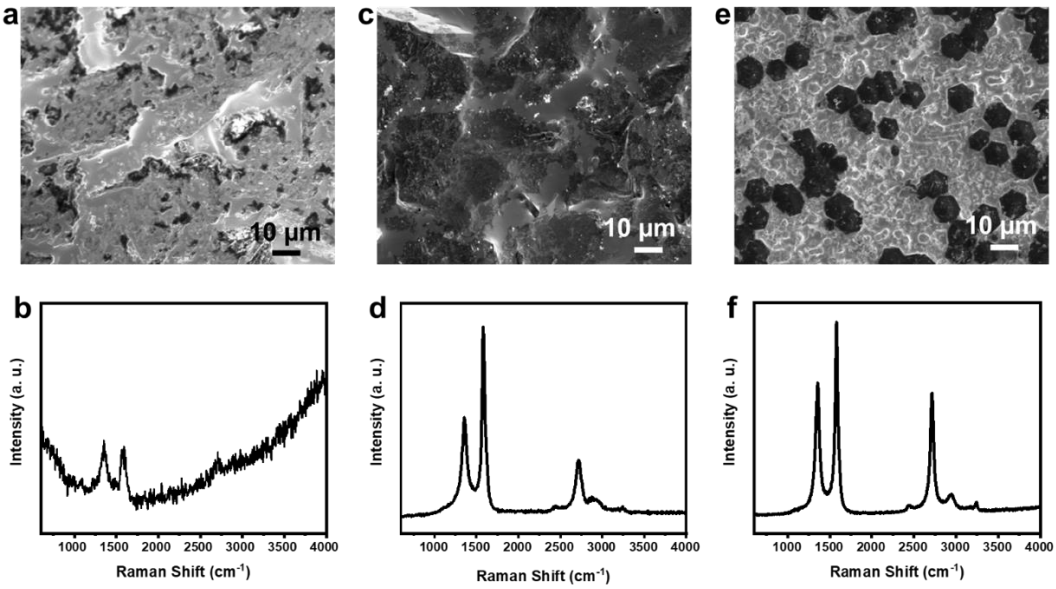

Figure R12. The experiment of Sn replacing Ga. The SEM image (a) and Raman spectrum (b) show the growth result for the liquid metal composed of 0.25 at% Si, 11.00 at% Ni, 11.00 at% Fe, 77.75 at% Sn. The SEM image (c) and Raman spectrum (d) show the growth result for the liquid metal composed of 0.25 at% Si, 11.00 at% Ni, 11.00 at% Fe, 38.87 at% Sn, 38.88 at% Ga. The SEM image (e) and Raman spectrum (f) show the growth result for the liquid metal composed of 0.25 at% Si, 14.67 at% Ni, 7.33 at% Fe, 38.87 at% Sn, 38.88 at% Ga.

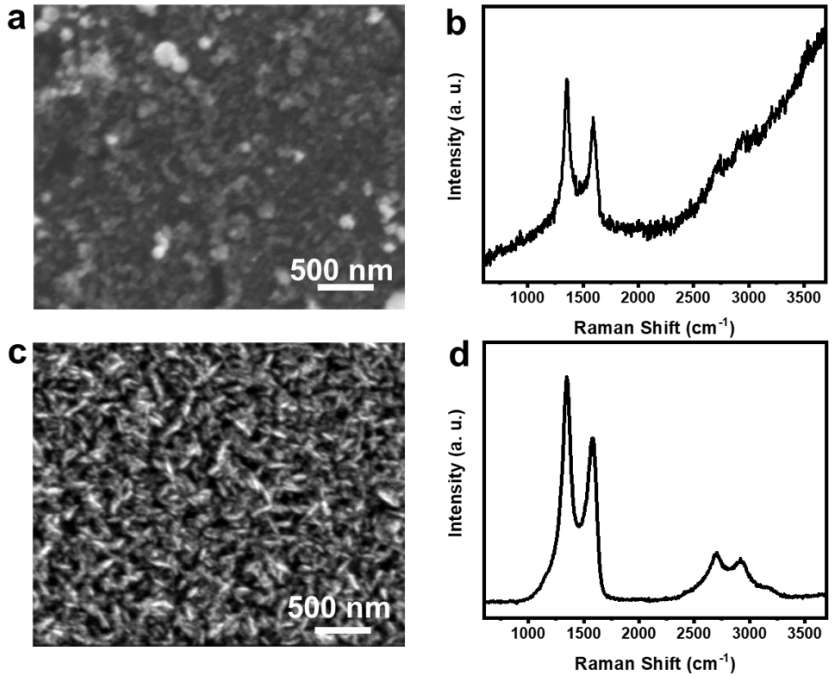

Figure R13. The experiment of In replacing Ga. SEM image (a) and Raman spectrum (b) show the growth result for the liquid metal composed of 0.25 at% Si, 11.00 at% Ni, 11.00 at% Fe, 77.75 at% In. SEM image (c) and Raman spectrum (d) show the growth result for the liquid metal composed of 0.25 at% Si, 11.00 at% Ni, 11.00 at% Fe, 38.87 at% In, 38.88 at% Ga.

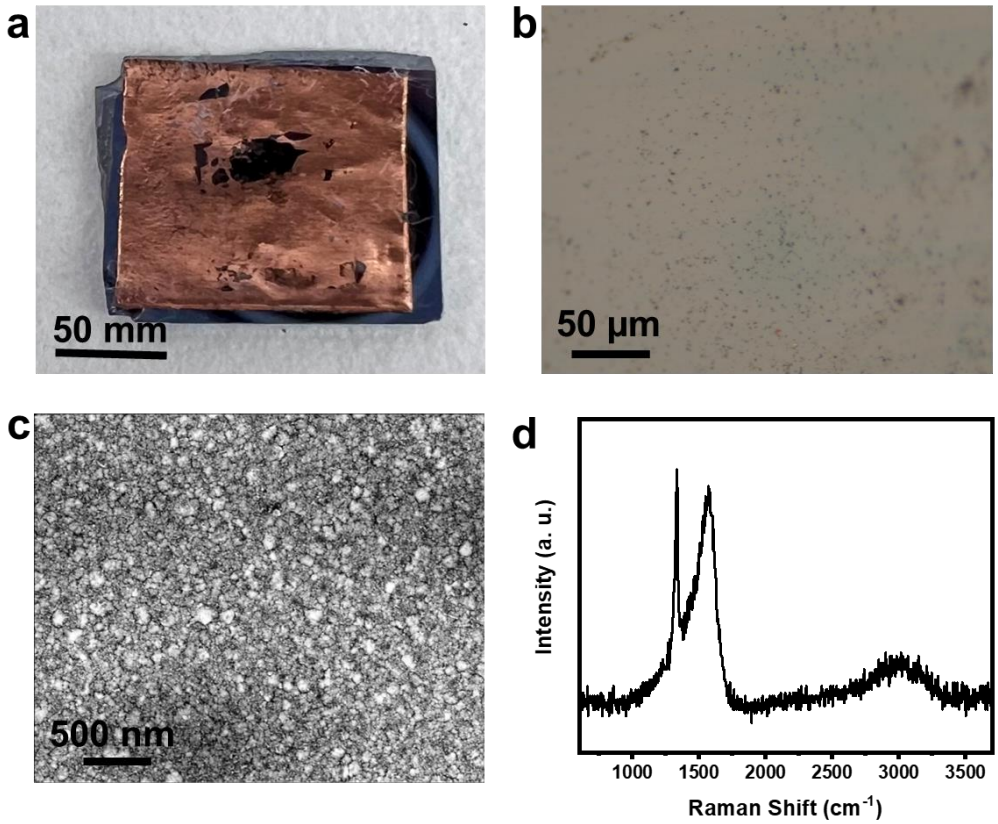

Figure R14. The growth result for the liquid metal composed of 0.25 at% Si, 14.67 at% Ni, 7.33 at% Fe, 38.87 at% In and 38.88 at% Ga. The photograph (a), optical microscope image (b), SEM image (c) and UV raman spectrum of as-grown diamond film transferred by Cu tape that was "sticked onto" the silicon wafer.

7. I think that the process is made unnecessarily complicated by using a graphite crucible which apparently is a source of carbon along with methane. It would be helpful to repeat some of these experiments with a quartz crucible.

Response:

Thank you for this suggestion.

We have tried a variety of other substrates, among them quartz (ST-cut, single crystal) and sapphire (c-plane, single crystal) substrates placed between the liquid metal and the bottom surface of our graphite crucible. We found quartz and sapphire reacted with the liquid metal by examining them after a typical growth run (Fig. R15). The growth with quartz substrate showed deposition of silica on the solidified liquid metal piece surface (Fig. R15a-b) and significant etching of the quartz surface (Fig. R15c). For sapphire, we observed deposition of alumina on

the surface of solidified liquid metal piece and etching of the sapphire surface (Fig. R15d-f).

We next tried placing a pyrolytic boron nitride (PBN) plate (5 mm x 5 mm x 1mm, MTI Korea) at the bottom of the graphite crucible between the liquid metal and graphite crucible. The PBN surface was not etched during our growth (it looks equally smooth as prior to the run). A diamond film of rainbow color was found on the solidified liquid metal surface (Fig. R16). SEM EDS showed no B or N in the diamond.

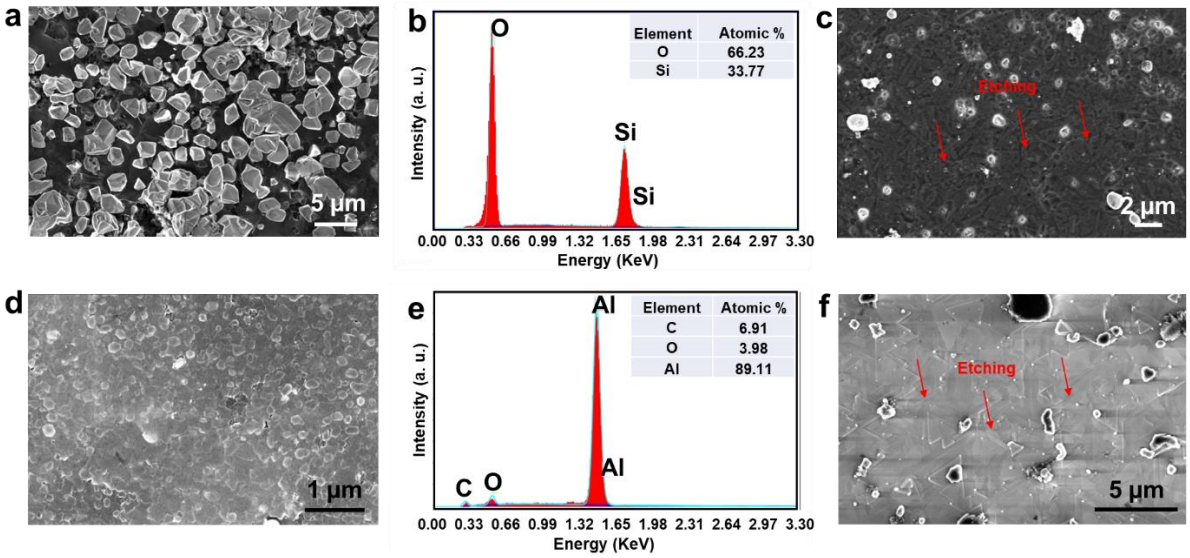

Figure R15. Growth runs with quartz or sapphire substrates placed between graphite crucible and liquid metal. (a) SEM image of SiO_2 crystal deposited on the solidified metal piece. (b) EDS spectrum of the crystal in a. (c) SEM image shows etching of the quartz substrate. (d) SEM image of Al_2O_3 crystals deposited on the solidified metal piece. (e) EDS spectrum of the crystal in d. (f) SEM image shows etching of the sapphire substrate.

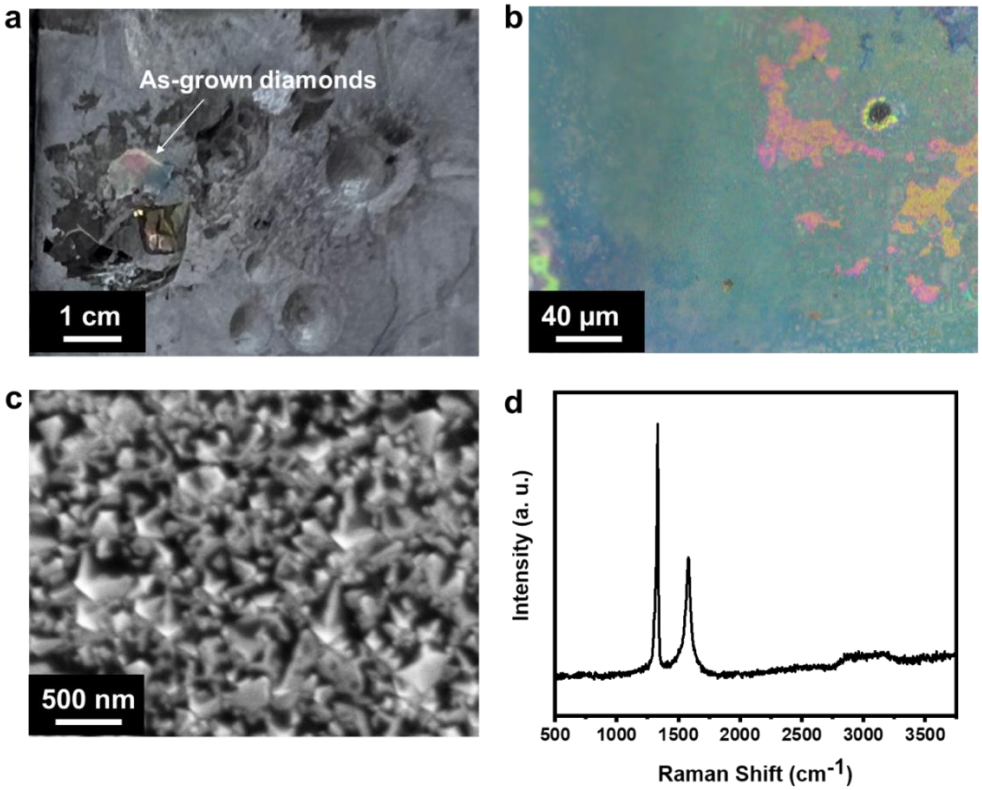

Figure R16. A growth run with a PBN (pyrolytic boron nitride) plate placed at the bottom of graphite crucible (thus between the liquid metal and graphite crucible). (a) Photograph shows the as-grown diamond region. Optical microscope image (b), SEM image (c) and UV Raman spectrum (d) of the as-grown diamond in (a).

8. The Upham paper (cited in the manuscript) showed that in the catalytic decomposition of methane by molten metal alloys the carbon produced by reaction dissolves in the melt. It would be good to know if this is the case here. This could be a carbon source for diamond growth.

Response:

Thank you for noting this.

We did 4 'growth runs' with $^{13}CH_4$ and H_2 for, respectively, 5 min, 10 min, 15 min, and 150 min.

We delaminated (by using a double-side copper tape) the entire bottom surface of the SLM for the 150 min run, thereby 'uncovering' the metal region that was underneath the as-grown diamond film ("M_D"), and another metal region ~ 5 mm away that did not have diamond grown on its surface ("$M_{Non\text{-}D}$"; please see Fig. R17a), but where there was some graphite. We note that we did not find diamonds grown for the 5 min and 10 min exposures to $^{13}CH_4$ and H_2. For

these two cases, "$M_{center\text{-}no\ D}$" refers to the center region but with no diamonds present (this center region is where diamonds are typically found on the SLM piece for longer growth times such as our standard 150 min, but also 15 min, 30 min, etc). We then used ToF-SIMS depth-profiling to study the concentration of carbon for the $M_{center\text{-}no\ D}$ and $M_{Non\text{-}D}$ regions for the 5 and 10 minute 'growth' runs, and the M_D and $M_{Non\text{-}D}$ regions for the 15 and 150 min 'growth runs'.

The center regions and "Non-D" regions show ^{13}C for all 4 samples. The concentration of ^{13}C, [^{13}C], was calculated by using a reference sample: A single crystal Ni(111) foil uniformly loaded with 0.77 at% ^{13}C.

Briefly, a "home-made" single crystal Ni(111) foil (100-μm-thick, see, e.g., *Science* 362,1021(2018)) was exposed at a high temperature in a Joule heating system (that also allows for extremely rapid cooling of the foil piece) to $^{13}CH_4$ gas to "dissolve" ^{13}C into the Ni(111) foil, and from the weight change of the foil before and after feeding with ^{13}C, a Ni(111) foil containing 0.77 at% ^{13}C was obtained with all ^{13}C in its interior and essentially none on the surface of this foil ^{13}C. We then did ToF-SIMS depth-profiling of this foil and found that the $^{13}C^-$ ion signal is 15.3x stronger than the Ni^+ ion (uniformly 15.3, for all isotopes of Ni) signal. We then used this pre-factor of 15.3 to calculate the [^{13}C] from the intensities of ^{13}C and Ni measured on/in our solidified liquid metal pieces, because the solidified liquid metal pieces have the known percentage of 11.00 at% Ni.

For the 5 min run (Fig. R17b), we found ^{13}C present in the metal subsurface and down to a depth of ~100 nm for both regions, and $M_{Non\text{-}D}$ (~26 at% at surface) has slightly higher ^{13}C concentration, [^{13}C], than $M_{center\text{-}no\ D}$ (~18 at% at surface). The [^{13}C] of both regions decreases to close to zero for depths larger than 100 nm.

For the 10 min run (Fig. R17c), the [^{13}C] in the $M_{center\text{-}no\ D}$ is ~65 at% at surface, and $M_{Non\text{-}D}$ is ~60 at% at surface. For the depth of ~10 nm at beginning, the [^{13}C] in $M_{Non\text{-}D}$ is very similar to $M_{center\text{-}no\ D}$. From the depth of ~ 10 nm to the final depth of 300 nm, the [^{13}C] in $M_{Non\text{-}D}$ is higher compared to $M_{center\text{-}no\ D}$.

For the 15 min run (Fig. R17d), the [^{13}C] at the surfaces of M_D and $M_{Non\text{-}D}$ regions are ~27 at% and ~18 at%, respectively.

Thus, at 10 min no diamonds have grown, but diamond had clearly grown by 15 min. The significantly smaller [^{13}C] found subsurface in the SLM regions following the 15 min run, compared to the 10 min run, is very likely (it essentially must be) due to the nucleation and growth of diamonds that consumes the ^{13}C (and generally for runs with normal methane: that consumes the subsurface carbon) inside the liquid metal.

The larger [^{13}C] of the M_D region compared to the $M_{non\text{-}D}$ region as a function of depth for the 15 min run suggests why diamonds are found where they are in our growths: We suggest that growth occurs in the central region at the bottom of the liquid metal contacting the EDM-3 sheet due to a lateral gradient in the concentration of dissolved carbon (here, studied with ^{13}C), and that this C concentration gradient inside the liquid metal at its bottom (sub-surface) region is likely created by the temperature gradient (measured with inserted thermocouples as described Fig. S2 in Supplementary Information), and possibly additionally contributed to by geometric factors (the geometry of our crucible). That is, a "flow" of dissolved C is generated towards the region where diamond nucleates, grows, and merges into a polycrystalline film.

And that under our growth conditions, the concentration of subsurface C atoms at about 10 minutes is so high that the supersaturation is very close to nucleating diamonds. **Nucleation evidently occurs followed by rapid growth of diamond particles between about 10 minutes, and less than 15 minutes.**

For the 150 min run (a polycrystalline diamond film formed; see Fig. R17e), the [^{13}C] at the surfaces of M_D and $M_{Non\text{-}D}$ regions are ~18.5 at% and ~20.5 at%, respectively, and the [^{13}C] of M_D and $M_{Non\text{-}D}$ are very similar for all depths to a depth of 300 nm.

Our TEM-EDS results (in our as-submitted manuscript) showed that the concentration of C in the SLM piece after a 150 min growth (TEM-EDS, Fig. 3d, Fig. S38; of cross sections made with SEM FIB cutting; that is, the "M1" region) was high in the subsurface region to a depth of ~30 nm, with ~26.5 at% at the SLM region directly adjacent to the diamond film. This value is close to the value now measured by using ToF-SIMS (~18.5 at% at the surface; see Fig. R17e).

We further note that the ToF-SIMS depth-profiling shows that the subsurface region contains a relatively large concentration of ^{13}C even to a depth of ~100 nm (Fig. R17b-e) for the 5, 10,

15, and 150 min runs. Note that TEM-EDS has a threshold detection of ~1 at% and ToF-SIMS a threshold of ppm to ppb, thus the longer "tail" of decreasing [^{13}C] in the Tof-SIMS depth-profiling. **What is important is that these two independent experimental methods (ToF-SIMS and TEM-EDS) show a high percentage of C in the near surface and 'sub-surface' regions. *This sub-surface region is where the diamonds nucleate and grow.***

SEM images show almost all diamond crystals are partially submerged in the SLM (at the early stages of growth, prior to when they have merged to make a film: such as for growth times of 15 and 30 min. For the single diamond particles that are partially submerged (in the, then, *solidified* liquid metal piece), where their apex is/are exposed (Fig. R18), has much higher brightness (due to diamond being insulating) than the submerged regions (that are surrounded by conductive metal). These SEM images *very strongly* suggest that nucleation and growth occur subsurface when the [C] reaches a critical level in the growth region (this central region), and C flowing towards the growth region from the surrounding regions feeds further growth as mentioned above.

Our new experimental results strongly suggest that the sub-surface carbon dissolved in the liquid metal nucleates and grows diamonds. **This strongly differentiates our growths (nucleation and diamond growth *inside* this liquid metal), from PE-CVD (plasma enhanced chemical vapor deposition) and HF-CVD (hot filament CVD) growth on solid substrates.**

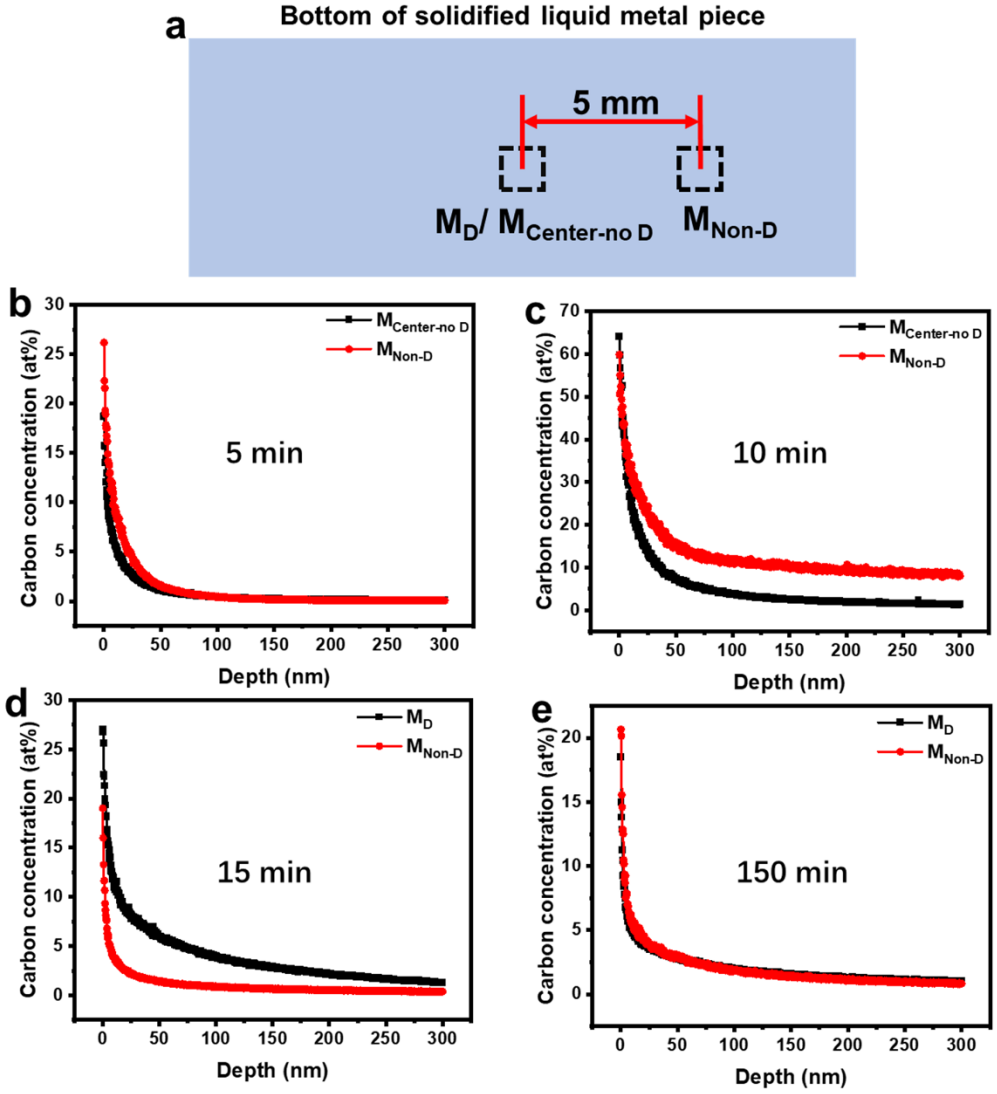

Figure R17. ToF-SIMS depth-profiling of carbon ($^{13}C^-$) concentrations obtained on two different regions of the solidified liquid metal (SLM) pieces. (a) A scheme showing the two regions of solidified liquid metal piece that we investigated. (b-e) ToF-SIMS depth-profiling of the two regions on solidified liquid metal pieces after growth for (b) 5 min, (c) 10 min, (d) 15 min, and (e) 150 min.

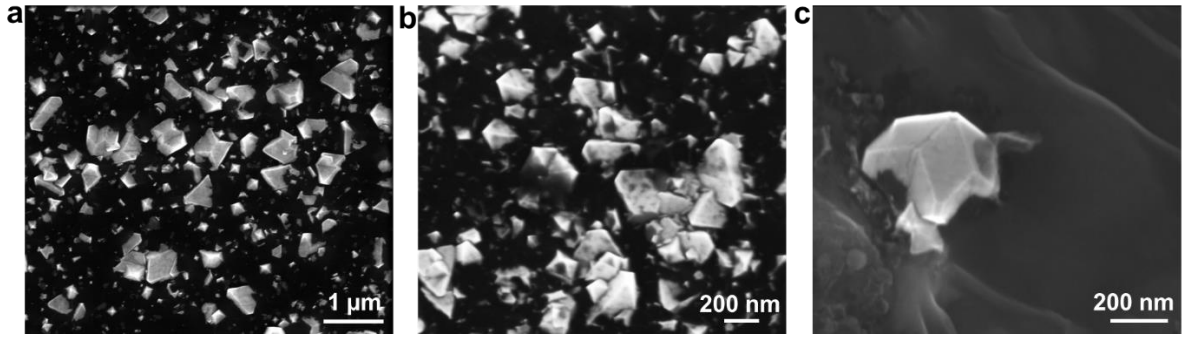

Figure R18. SEM images showing as-grown diamonds 'buried' (partially) in solidified liquid metal after a growth of 30 min.

9. Minor points:

Lines 33, 34: “synthesize diamonds from melted iron sulfide”. This is an alchemist’s dream. The authors probably meant “synthesize diamonds by using a molten iron sulfide catalyst”.

Response:

Thank you. Corrected.

Line 44: replace “The new growth diamond” with “The diamond grown in this way”.

Response:

Thank you. Corrected.

Line 64: “It is reported that liquid metal acts as catalyst to dissolve carbon”. I would prefer “molten metal acts as a solvent that dissolves carbon”

Response:

Thank you. Corrected.

Lines 74-76: A statement was made that liquid metals are good catalysts because they have an abundance of electrons and ions. Solid metals have the same abundance of electrons and ions as the liquid ones. Please remove those lines.

Response:

Thank you. Removed.

Referee #2 (Remarks to the Author):

Natural diamonds obtained from the earth is thought to grow in a high pressure and high temperature (HPHT) condition, while synthetic diamond can be produced by both HPHT methods (with or without using metal catalyst) and chemical vapor deposition (CVD) processes

at atmospheric pressure or lower pressure. In this work, the authors present a new process for the synthesis of diamond in liquid metal with Ni, Fe and Si addition at 1 atmosphere pressure. The study carried out here is systematic, different parameters for diamond growth have been examined and the products are also well characterized. In fact, the synthesis of diamond at ambient pressure or pressure lower than 1 atmosphere is not novel since CVD methods already realize this goal and it is well developed now. The new method for diamond growth presented here by using liquid metal sounds interesting which may present new insight on the diamond growth mechanism but the underlying mechanisms are far from being understood, which however, is important for this work and needs to be uncovered. Besides this, there are also some issues need to be addressed.

Response:

Thank you for reviewing our paper. We have delved more deeply into growth mechanisms by doing additional experiments and from theoretical modeling. Please see our responses to your comments further below.

1a. For the diamond growth with CVD process, carbon precursor, for example, CH_4/H_2, is decomposed and then act as carbon source for diamond crystals/films formation. In this case, either a diamond seed or a substrate (such as Si, Mo and Iridium modified substrate) is used for diamond growth. There are similarities between CVD and the process reported here, such as high temperature condition, and the same carbon source. Thus, the CVD for diamond synthesis should also be mentioned in the background introduction and even compared with their result discussion, such as growth mechanism.

Response:

Thank you for your comment. Please see the 1st section in the RESPONSES ON TWO TOPICS TO ALL REVIEWERS on Pages R1-R4.

We have added descriptions of CVD growth methods in the Introduction.

1b. For the diamond growth mechanism, most discussion is based on speculation. I strongly suggest an atomic level understanding of the diamond formation mechanism by theoretical simulation, to show how the graphite crucible (but not other carbon source) and the decomposed CH_4 transform into diamond in liquid metal. This is very important and would be very helpful to improve the work.

Response:

Thank you for your comment. Please note the 2nd section in the RESPONSES ON TWO TOPICS TO ALL REVIEWERS on pages R4-R5, and thus our **current** emphasis on the use of the EDM-3 graphite piece and the growth of diamonds from methane. The EDM-3 plate does not contribute carbon to the diamond growth. The diamonds grown from the methane are higher quality. We have thus chosen to focus on always using the EDM-3 plate between the crucible graphite and the liquid metal. We were thus performing the theoretical simulations to understand the growth mechanisms of diamonds from methane including the possible roles of Si (please see our simulation results described further below), and we believe that the mechanism of diamond growth from graphite crucible carbon could be explored in the future either by us or others who read our paper.

We have added 5 new coauthors, namely Prof. Geunsik Lee, and his group members Drs. Babu Ram, Mohammad Zafari, and Yongchul Kim, and graduate student In Kee Park, who have undertaken extensive modeling of certain species in the liquid metal, and of the activation of CH_4 at the surface of the liquid metal.

i) Activation of methane by liquid metal

As mentioned, the ToF-SIMS depth-profiling data always shows the highest concentration of C atoms closest to the surface of the SLM pieces after all runs (5, 10, 15, 30, etc, to 150 min).

We have thus calculated the activation of methane (CH_4) as it might happen at the liquid metal (LM) surface (gas/liquid interface) with C-H bond dissociation yielding CH_3 and H radicals adsorbed at the liquid metal surface.

The radial distribution function (RDF) of the liquid Ga structure was obtained by ab initio

molecular dynamics (AIMD) simulation at 375 K and 1300 K as shown in Fig. R19. The highest peak at 375 K (~2.7 Å) decreased at 1300 K, due to the formation of low-coordinated atoms at the surface. Per our computational study the liquid Ga surface structure is disordered at high temperature (1300 K) and small clusters appear and disappear dynamically. In this regard, we note a computational study of the Indium (In) liquid surface at 1200 K that reported small surface clusters playing a critical role for dissociation of the first C-H bond in methane adsorbed on the liquid indium surface (*J. Phys. Chem. A* 123, 8907 (2019)).

We found that the C-H bond dissociation energy on a solid Ga slab is 0.83 eV (Fig. R20; note that this is a zero Kelvin calculation, thus E (calculated electronic energy) values are shown). Of course, the liquid metal is not crystalline gallium, but we note this low value as interesting.

To probe possible CH_4 activation at the surface of the liquid Ga-Fe-Ni mixture, Ga, Ga-Ga (dimer), and Fe and Ni atoms, were considered as individual entities, and then Ga and Ga-Ga were also located on top of a particular mixture of Ga-Fe-Ni as described further below. The overall reaction of interest is:

$$CH_4(g) + \text{cluster} \rightarrow CH_3(ads) + H(ads) \qquad (1)$$

And we consider Reactions (2) and (3) that yield Reaction (1):

$$CH_4(g) + \text{cluster} \rightarrow CH_4(ads) \qquad (2)$$

$$CH_4(ads) \rightarrow CH_3(ads) + H(ads) \qquad (3)$$

in which “ads” means “adsorbed”, and the energy changes are ΔE_1 and ΔE_2 for Reactions (2) and (3), respectively (or ΔH_1 and ΔH_2, or ΔG_1 and ΔG_2, as discussed below).

The adsorption free energies of methane (ΔG_1) on different clusters are shown in Table R1 and R2, in which $G(CH_4(ads))$ is the (Gibbs) free energy of the CH_4 adsorbed on the cluster, $G(CH_4)$ the free energy of CH_4 in the gas phase, and G(cluster) is the free energy of the ‘cluster” such as (Ga atom, Ga dimer, Fe atom, Ni atom; or these atop of Ga_9FeNi as described below). CH_4 can be adsorbed on an Fe atom in the quintet spin state at -0.60 eV, indicating strong orbital hybridization. For other clusters, methane is physiosorbed on the surface with a weak binding energy.

So that we are comparing "apples to apples" and not "apples to oranges" we briefly discuss the meaning of ΔH and ΔG to correctly account for the dramatic impact of adsorption on changing ΔH, compared to the gas phase reaction. The gas phase reaction ΔH and ΔG values are shown below (Screen Save from HSC Chemistry. HSC Chemistry is a software package including highly accurate thermochemical data; https://www.hsc-chemistry.com/):

Reaction Equation					
CH4(g) = CH3(g) + H(g)					
Reaction Data					
T °C	ΔH kJ	ΔS J/K	ΔG kJ	K	Log K
800.000	449.710	142.918	296.338	3.757E-015	-14.425
900.000	450.063	143.233	282.029	2.764E-013	-12.558
1000.000	450.251	143.388	267.697	1.038E-011	-10.984
1100.000	450.296	143.422	253.355	2.299E-010	-9.638
1200.000	450.208	143.361	239.015	3.345E-009	-8.476
1300.000	449.995	143.222	224.685	3.459E-008	-7.461

One notes that the ΔH values are almost invariant. Because of the large contribution to the translational entropy by having 2 gas phase species (CH_3 and H) on the right-hand side of the chemical equilibrium, and 1 gas phase species on the left-hand side (CH_4), comparing our calculated values of ΔG for *adsorbed* CH_4, CH_3, and H to the gas phase ΔG values, inappropriately favors this large ΔS_{trans} contribution in the gas phase. It is for this reason that we discuss our calculated **ΔH** values below so that they can be compared to the 450 kJ/mol (i.e., 4.66 eV) gas phase ΔH value. Thus, it is the change in endothermicity due to the methane-liquid metal interaction, that is relevant, by comparing our calculated $\Delta H_1 + \Delta H_2$ to the gas phase endothermicity of ΔH = 4.66 eV.

The C-H bond dissociation (the sum of ΔH_1 and ΔH_2 is the relevant energy change) can *readily* occur on Ga atom, Ga-Ga dimer, Fe atom, or Ni atom: The calculated C-H bond dissociation enthalpy values ($\Delta H_1 + \Delta H_2$, Table R1) are 0.50 eV (Ga atom), -0.27 eV (Fe atom), 1.64 eV (Ni atom), and 0.51 eV (Ga-Ga dimer). All values are *much smaller* than the gas phase bond dissociation energy of ~4.66 eV. Indeed, the calculated change in endothermicity for the reaction when the methane is considered as 'adsorbed' to these species, is remarkable.

Of course, Ga, or Ga-Ga, (or Fe or Ni) would have Ga-Fe-Ni liquid metal 'beneath' them; to include (as best we could) the role of this LM on C-H bond dissociation for surface adsorbed

CH_4, we made a periodic slab including Ga, Fe, and Ni atoms. A Ga_9FeNi cluster was 'cut out' of the fully optimized periodic Ga slab surface (the '100' surface of alpha-gallium) that was doped by Fe and Ni atoms placed in interstitial sites. The Ga, and Ga-Ga, were then placed 'atop' this Ga_9FeNi cluster. The Ga/Ga_9FeNi yielded a C-H dissociation enthalpy value of -0.11 eV and Ga-Ga/Ga_9FeNi a value of 2.75 eV. These values are also significantly lower than 4.66 eV. (We did not pursue Fe or Ni atop this Ga_9FeNi cluster due to computational complexity.)

Our computed values for gas phase methane being adsorbed and then converting to adsorbed methyl radical and adsorbed H atom radical show that the experimental liquid metal should be remarkably activating of methane at the temperatures around 1300 K used in experiments.

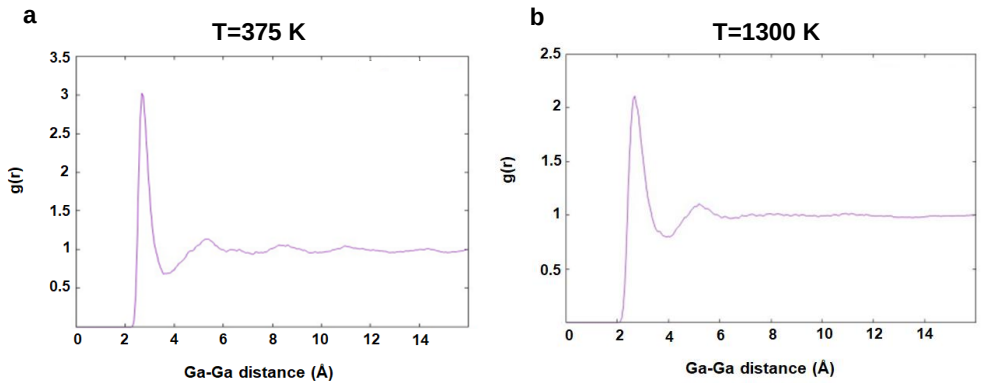

Figure R19. (a-b) Computed radial distribution function (RDF) of liquid Ga at (a) 375 and (b) 1300 K using AIMD trajectories.

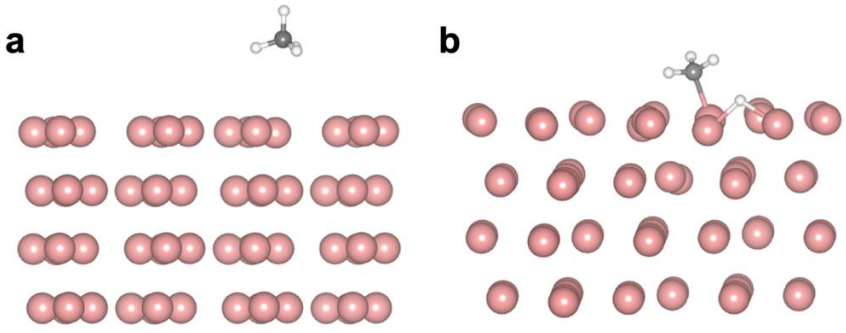

Figure R20. (a-b) Optimized structure of (a) CH_4(ads) and (b) CH_3(ads) + H(ads) on Ga slab surface (100), where ΔE_1 is -0.17 eV and ΔE_2 is 1 eV. All layers in the Ga slab were fully relaxed with VASP at 0 Kelvin.

Table R1. Calculated CH_4 adsorption free energy (ΔG_1: G(CH_4(ads)) – G(CH_4) – G(cluster)) and bond dissociation energy of adsorbed CH_4 (ΔG_2: G(CH_3(ads)) + G(H(ads)) – G(CH_4(ads))) on different clusters. The $\Delta G_1 + \Delta G_2$ is the overall Gibbs free energy change of the reaction

(CH_4(g) + cluster → CH_3(ads) + H(ads)). The change in enthalpy for each reaction is also shown, ΔH_1 and ΔH_2. All calculations were performed with Gaussian in which electronic energy was obtained by the MP2 method. Atom positions were kept fixed in Ga_9FeNi during optimization while Ga or Ga-Ga atop Ga_9FeNi were optimized. The temperature was set to 1300 K.

Reactant State	CH_4(ads)	CH_3(ads) + H(ads)	ΔG_1(eV) ΔH_1(eV)	ΔG_2(eV) ΔH_2(eV)	$\Delta G_1+\Delta G_2$ (eV) $\Delta H_1+\Delta H_2$ (eV)
Ga	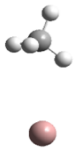	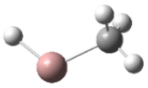	0.96 0.23	0.58 0.27	1.54 0.50
Fe		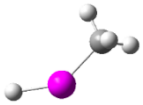	-0.60 -1.52	1.06 1.25	0.46 -0.27
Ni	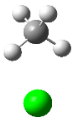	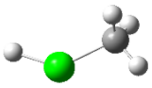	1.60 0.56	1.07 1.08	2.67 1.64
Ga	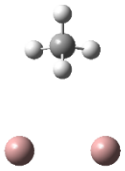	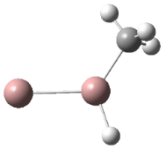	0.98 0.31	0.68 0.20	1.66 0.51
Ga	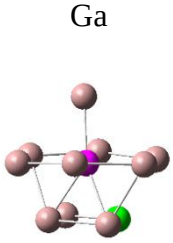	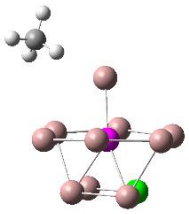	1.09 0.33	0.34 -0.44	1.43 -0.11
Ga-Ga	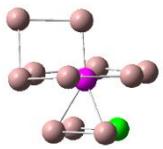	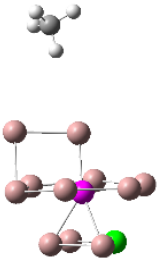	1.37 1.08	2.68 1.67	4.05 2.75

Table R2. Calculated electronic energy (E_e), zero-point energy (ZPE), entropy correction (-TS)

and thermal correction (U), where Gibbs free energy was obtained via $G= E_e + ZPE – TS + U$. The unit is a.u. and the temperature was set to 1300 K.

Species	E_e	ZPE	-TS	U (thermal correction)	$G = E_e + ZPE –TS + U$
CH_4	-40.33408	0.04401	-0.14256	0.02287	-40.40975
Ga	-1923.14743	0	-0.09799	0.00617	-1923.23925
CH_4(ads) on Ga	-1963.47907	0.04447	-0.21365	0.03465	-1963.61360
CH_3(ads) + H(ads) on Ga	-1963.4655	0.03931	-0.20228	0.03629	-1963.5922
Fe	-1262.29547	0	-0.10048	0.00618	-1262.38977
CH_4(ads) on Fe	-1302.69165	0.04510	-0.20893	0.03404	-1302.82144
CH_3(ads) + H(ads) on Fe	-1302.6417	0.03787	-0.21578	0.03727	-1302.7823
Ni	-1506.80815	0	-0.09859	0.00618	-1506.90057
CH_4(ads) on Ni	-1547.12702	0.04420	-0.20286	0.03430	-1547.25136
CH_3(ads) + H(ads) on Ni	-1547.08396	0.03868	-0.20343	0.03664	-1547.2121
Ga-Ga	-3846.34048	0.00037	-0.15568	0.01406	-3846.48174
CH_4(ads) on Ga	-3886.67344	0.04499	-0.27343	0.04642	-3886.85546
CH_3(ads) + H(ads) on Ga-Ga	-3886.66291	0.04116	-0.25580	0.04722	-3886.83034
Ga/Ga_9FeNi	-22001.49460	0.00043	-0.24494	0.02426	-22001.7148
CH_4(ads) on Ga/Ga_9FeNi	-22041.8284	0.045113	-0.359966	0.058743	-22042.08451
CH_3(ads) + H(ads) on Ga/Ga_9FeNi	-22041.84116	0.04147	-0.33145	0.05911	-22042.07203
CH_3(ads) + H(ads) on Ga/Ga_9FeNi	-23924.79256	0.00136	-0.28110	0.035728	-23925.03657
CH_4(ads) on Ga-Ga/Ga_9FeNi	-23965.0992	0.04580	-0.41309	0.07049	-23965.3960
CH_3(ads) + H(ads) on Ga-Ga/Ga_9FeNi	-23965.03437	0.041873	-0.37633	0.07114	-23965.29769

Experimental E_A values for pure gallium activating methane.

Wi, et al., recently reported (*Chemical Engineering Journal* 460, 141558 (2023)) the activation energy for the decomposition of methane on an electrostatically levitated droplet of liquid gallium (and the same for droplets of molten In, Sn, Bi, and Cu). They measured the rate of production of hydrogen gas upon introduction of a 10 vol% methane, 90 vol% argon gas mixture, at a set of different temperatures in the temperature range shown below (Fig. R21; where we have cut and pasted their Table 6). Their temperature range encompasses our measured temperatures in the region where diamond grows, and nearby that region at the bottom of the liquid metal near the cavity bottom, per our inserted thermocouple measurements. Many of our theoretical values (Table R1) for a variety of possible surface species for Reaction (3), have a change in enthalpy value indeed *below* 115.3 kJ mol^{-1} (1.19 eV) the E_A value shown in Fig. R21. We note that. per the authors, the levitated gallium droplet had a mass of 0.5 g, and with the density of gallium at 1300 K being about 5.5 g/cm^3, this 1/11 cm^3 spherical droplet has (our calculated values) a diameter of 0.56 cm and surface area of 0.98 cm^2.

Table 6
Activation energy and pre-exponential factor of the Arrhenius plot shown in Fig. 7.

	E_A (kJ mol^{-1})	ln k_0 (m s^{-1})	Temperature range (°C)
In	198.6 ± 19.4	11.1 ± 1.8	948–1140
Ga	115.3 ± 12.5	3.6 ± 1.2	849–1132
Bi	315.9 ± 21.2	21.6 ± 1.9	880–1221
Sn	318.2 ± 28.0	20.6 ± 2.4	1021–1220
Cu	240.3 ± 3.7	13.5 ± 2.0	1095–1238

Figure R21. Screen capture of Table 6 in "*Chemical Engineering Journal* 460, 141558 (2023)".

The authors noted in their paper that: "*Full electromagnetic levitation could be applied to the conductive materials, because of which this technique is expected to be suitable for use with other metals. The technique will not be limited to pure metals, as shown in the present study, but can be extended to metal alloys composed of more than one element. Indeed, the authors have already performed the pyrolysis of methane gas on molten metal alloys composed of 2 or 3 elements, using the developed levitation technique. The results will be reported elsewhere.*" We've just recently (December 19) contacted the team at POSTECH, "just up the

road from us at IBS CMCM and UNIST" to learn more about their experiments and to discuss whether our alloy could be tested.

We note, also, the study by Fujita, et al. (*Scientific Reports* 7, 12371 (2017)), in which they fit rate data for the decomposition of methane, in their study of very low temperature growth of graphene onto the edges of pre-existing (~1 μm lateral dimension) graphene "seeds" on sapphire or polycarbonate surfaces. The obtain E_A values for methane decomposition as they describe here, where we quote verbatim: "*The Arrhenius plot shows two temperature windows with distinct energy barriers, i.e., a high-temperature region >500 °C with an activation barrier E_a of ~0.58 eV and a low-temperature region <300 °C with an activation barrier E_a of ~0.16 eV. The window between 300 °C to 500 °C is a transition range in which processes associated with the two above barrier values are both contributing. The E_a ~0.58 eV barrier is consistent with the reported values from 0.52 eV to 0.77 eV obtained with a Ni catalyst. However, the observed low E_a ~0.16 eV for the low-temperature graphene edge growth is surprising. It suggests that a simple methane activation process is unlikely valid. Instead, parallel processes could be competing in the molten gallium catalyst, particularly at a lower temperature.*" For convenience: 0.58 eV = 56 kJ/mol; 0.16 eV = 16 kJ/mol.

ii) Role of Si

To try to provide a theoretical understanding of possible initial steps towards diamond formation in the liquid metal used in experiments, *ab*-initio molecular dynamics (AIMD) and density functional theory (DFT) electronic structure analysis were performed. The formation energy per atom at the initial stage was calculated to help understand the process of clustering of carbon dissolved in liquid Ga (that we sometimes refer to as "the solvent" but also as "pure liquid gallium" in the text). The formation energy per atom was calculated as:

$$E_{\mathrm{Formation}} = (E_{n\mathrm{C}+m\mathrm{Si}+\mathrm{solvent}} - E_{\mathrm{solvent}} - n\mu_{\mathrm{C}} - m\mu_{\mathrm{Si}})/(n+m),$$

where n and m refer to the number of carbon and silicon atoms in the liquid metal solvent, and $E_{n\mathrm{C}+m\mathrm{Si}+\mathrm{solvent}}$, E_{solvent}, μ_{C}, and μ_{Si} indicate the *total energy of the solution*, the *energy of the solvent* (the liquid gallium), and the *chemical potential of C and Si*, respectively. The chemical potential of C and Si is the change in energy when each was added to the liquid

gallium solvent, namely,

$$\mu_{\mathrm{C/Si}} = (E_{\mathrm{C/Si}} - E_{\mathrm{solvent}}).$$

Figure R22a shows the formation energy of C_2, Si-C, Si-C-C, and C-Si-C per atom in two types of solvent, a pure liquid Ga and a liquid mixture of 120 Ga, 13 Ni, and 13 Fe atoms (denoted as Ga-Ni-Fe). For the pure liquid gallium case, each of C_2, Si-C, Si-C-C, and C-Si-C have a negative formation energy indicating these dimers or trimers are favored relative to the atomic species. For liquid Ga-Ni-Fe the formation energy was lowered from -0.37 to -0.63 for C_2, from -0.27 to -0.70 for Si-C-C, and from -0.09 to -0.73 for C-Si-C, in eV/atom; thus C_2, Si-C-C, and C-Si-C are substantially stabilized in liquid Ga-Ni-Fe. We note that Si-C was found to be dissociated at equilibrium in liquid Ga-Ni-Fe, which is attributed to a stronger Fe-C interaction than Si-C.

Regarding the effect of Si, the electrostatic interaction was found to lower the formation energies of Si-C-C and C-Si-C from a Bader charge analysis, as shown in Fig. R22b.

The electronegativity of a C atom ($\chi_{\mathrm{C}} = 2.55$) is higher than that of Ga, Ni, and Fe ($\chi_{\mathrm{Ga}} = 1.81$, $\chi_{\mathrm{Ni}} = 1.91$, and $\chi_{\mathrm{Fe}} = 1.83$), and indeed in the liquid Ga at 1300K the C atom has 0.97 more electrons on average than a neutral C atom. Si has an electronegativity ($\chi_{\mathrm{Si}} = 1.90$) similar to that of Ga and the Bader analysis shows only a small change in the number of electrons compared to a neutral Si atom.

In the C_2 dimer, a C-C covalent bond is found and the interaction with liquid Ga was found to be smaller, so the number of additional electrons for each carbon atom is reduced by 0.3 to 0.4 compared to the isolated C atom. For Si-C, the interaction between Si and C is weak, so mostly it remained in dissociated form, thus the number of electrons is close to that of the atomic case. However, when a Si atom contacts *two* C atoms, this Si atom supplies additional electrons to the neighboring C atom. In Fig. R22b, Si in the C-Si-C structure loses 1.3 electrons on average, and the two C atoms have 11.07 electrons. In the structure Si-C-C, $C_{(1)}$ directly bonded to Si has 5.03 electrons, whereas $C_{(2)}$ that is the second neighbor of Si has 4.55 electrons which is similar to the average number of electrons of C_2 without Si. The electron transfer from Si to C *rationalizes* the significantly lowered formation energies of Si-C-C and C-Si-C.

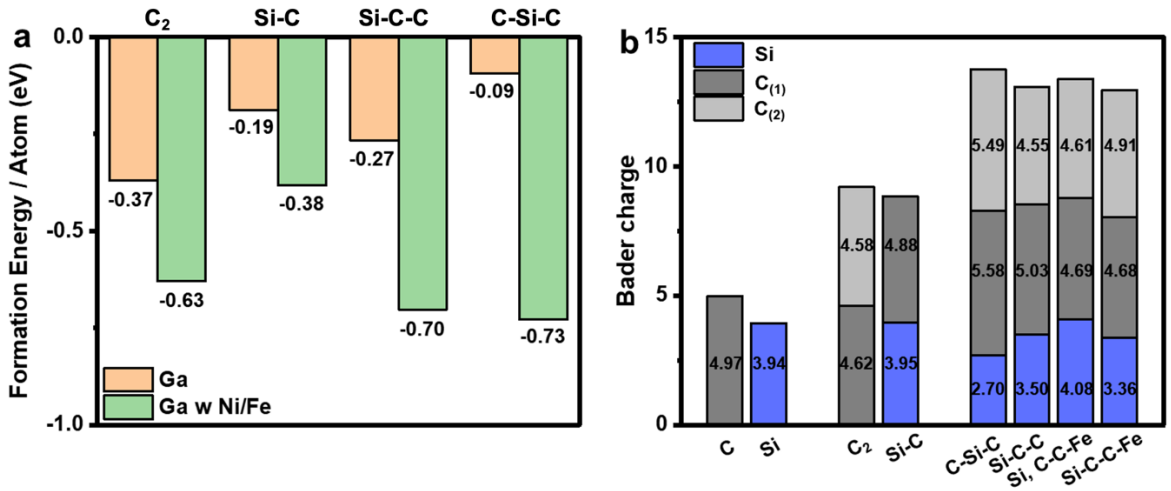

Figure R22. (a) Formation energy per atom in 120 Ga liquid metal (orange column) and in the Ga-Fe-Ni liquid metal (120 Ga, 13 Ni, and 13 Fe; green column). (b) The Bader charge for each species in the Ga-Fe-Ni liquid metal.

In addition, the interactions of Fe with C as C moves around in the Ga-Fe-Ni liquid metal contributes to lower the formation energies of C_2, Si-C-C, and C-Si-C as shown in Fig. R22a. An image of each species within the Ga-Fe-Ni liquid metal and its relative total energy is shown in Fig. R23, and we found that those with an Fe-C interaction have relatively lower total energies compared to those without such a Fe-C interaction. And as mentioned the formation energy is further lowered by the presence of Si in the cluster, note the two values in Fig. R23 for Fe-C-C (-0.49 eV) and Fe-C-C-Si (-0.92 eV), respectively.

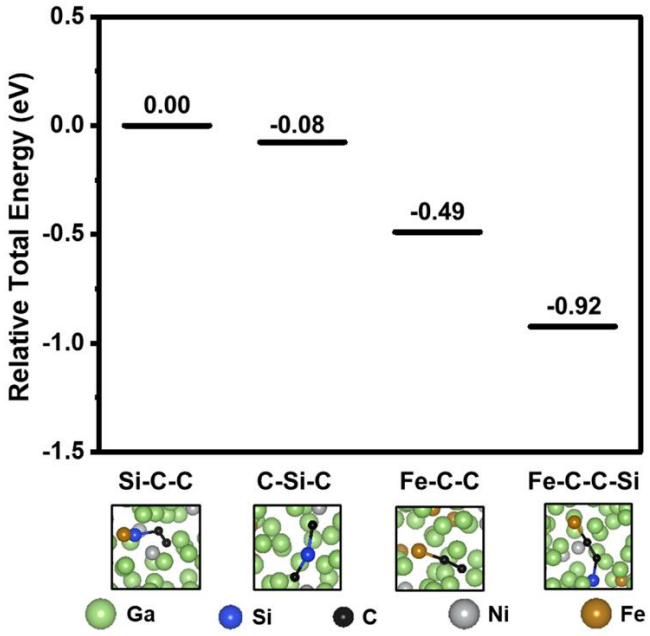

Figure R23. Relative total energies of Si-C-C, C-Si-C, Fe-C-C, and F-C-C-Si and their structures. There is one Si and two C in the Ga-Ni-Fe solvent in each case.

From our analysis of the formation energy and the Bader charge, a Si atom plays a special role in stabilizing such small clusters that are possibly the starting point of building larger clusters (this is discussed below) and finally, diamond nuclei.

Projected density of states (PDOS) analysis was done to further understand the formation energies and Bader charges (Fig. R24). Both C and Si atoms dissolve in liquid gallium, a metal having zero band gap and showing free electron behavior. In the C atom, the s-orbital maintained the local atomic state in the low energy region below -10 eV compared to the Fermi level, whereas the s-orbital of Si was also assimilated to the state of Ga and became broader like the p-orbital of Si. In addition, the projected DOS of the isolated single C atom and the C_2 dimer differed in s-orbital character in the low energy region. The C_2 dimer has a stable C-C covalent bond state around -15 eV relative to the Fermi level, and these states lower the C_2 formation energy. As mentioned above, in terms of formation energy, Si showed greater stability when connected to two C atoms than when interacting with a single C atom, and the projected DOS results also support this. The bond between Si and a single C atom was weak, and the orbital overlap was minimal. When Si is connected to two C atoms (Si-C-C, C-Si-C), the orbital overlap is greatly improved through the formation of a bond with C in the low energy

region. Compared to the C-C bond state of the C_2 dimer, the energy level of the carbon bonding state of Si-C-C moved to a lower value.

This is the reason why Si strengthened the C-C bond and the Si-C-C structure has a significantly lower formation energy. The projected DOS of the Fe-C-C and Fe-C-C-Si structures show that the interaction between Fe and C is related to the p-orbital around -1 eV compared to the Fermi level. The gray area in Fig. R24g-h shows that the C in direct contact with Fe overlaps with the states of Fe, slightly increasing the p-orbital DOS. Among other MD simulations, there was a case where C was surrounded by transition metals, and the p-orbital of C, which was broad (highly delocalized "into" the surrounding liquid gallium) due to interaction with the neighboring Ga atoms; in this case of neighboring Fe and Ni atoms as well as Ga atoms, we find a fairly high peak and local properties (Fig. R25). This result also indicates that Fe and Ni (and likely some of the other transition metals, such as Co) mainly interact with the p-orbital of C for a liquid metal mixture composed of 120 Ga, 13 Fe, and 13 Ni atoms.

To study the role Si plays, a moderately large number of C atoms were dissolved in the liquid Ga-Fe-Ni with and without Si atoms, and the MD trajectories were studied. For no Si, the unit cell in the slab model contains 120 Ga, 13 Ni, 13 Fe, and 15 C, and in the first part of the MD trajectory of 18 ps (Supplementary Movie 1), C_3 was the largest size of C cluster formed. We then added another 5 C atoms (making 20 C in total) and performed a second MD of 16 ps (Supplementary Movie 2). Likewise, in the presence of Si, a first MD of 15ps was performed with 15 C and 5 Si atoms dissolved in the Ga-Ni-Fe liquid metal (Supplementary Movie 3), and after adding 5 more C atoms, an additional MD of 16ps was then done (Supplementary Movie 4). In the case without Si, no carbon structure larger than C_3 was found in both the first and second runs of MD (Supplementary Movie 1 and 2, Figure R26a). However, in the presence of Si atoms, Si-C-C, C-Si-C, and C_3 structures were formed in the initial MD, and after additional C atoms were supplied, a cluster containing tetrahedral Si and multiple carbon atoms was formed within 10 ps (Fig. R26b) and stabilized a carbon cluster (Supplementary Movie 4, Fig. R26c).

PDOS were obtained for the final structures of MD in the presence and absence of Si, respectively (Fig. R27a-b). When there is no Si, electronic states corresponding to several C_2

dimers or C_3 chains appeared (Fig. R27a), and in the Ga-Fe-Ni liquid metal with Si atoms, many bonding states appeared between Si and C (Fig. R27b). In particular, the p-orbital state of carbon between -10 and -5 eV increased due to the influence of Si; this means that the p-orbitals of the carbon cluster are localized in that energy level. In addition, the observed tetrahedral Si showed an electronic state close to sp^3, showing formation of this sp^3-bonded when Si atoms are present (Fig. R27c).

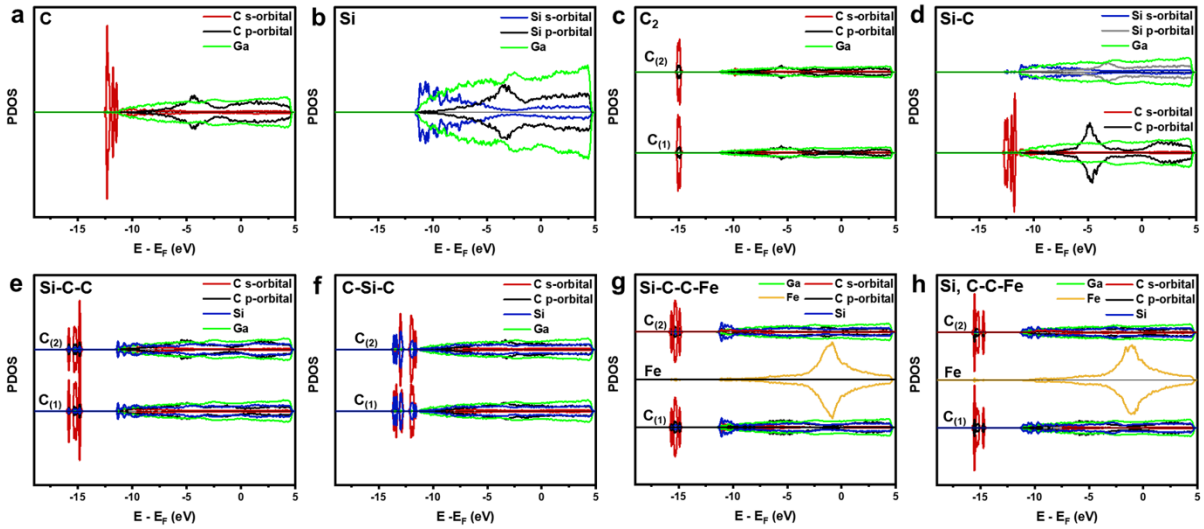

Figure R24. Projected DOS of the indicated clusters. (a-b) PDOS for a single atom in Ga-Ni-Fe solvent: (a) C and (b) Si. (c-d) PDOS is presented for: (c) C_2 and (d) Si-C. (e-h) PDOS of (e) Si-C-C, (f) C-Si-C, (g) Si-C-C-Fe, and (h) C-C-Fe (with isolated Si). The s-orbital and p-orbital of carbon are shown in brown and black, respectively. In (b) and (d), the s-orbital and p-orbital states of Si are shown in blue and gray, respectively, but in (e), (f), (g), and (h), the Si state is shown in blue. In a two-carbon structure, the first carbon is denoted as $C_{(1)}$ and the second carbon is denoted as $C_{(2)}$, respectively, and the Fe state bonded to carbon is shown in orange in (g) and (h). The gray area in (g) and (h) shows the states where Fe and C overlap and form bonding states. PDOS is the result of summing each element type and dividing by the number of elements.

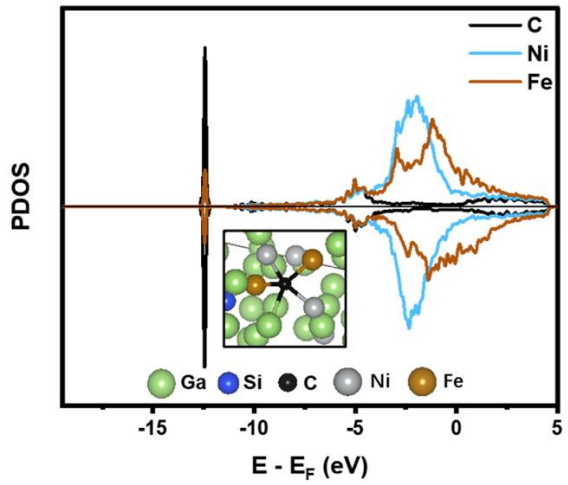

Figure R25. Projected DOS and its structure when carbon interacts with many surrounding Ni and Fe atoms.

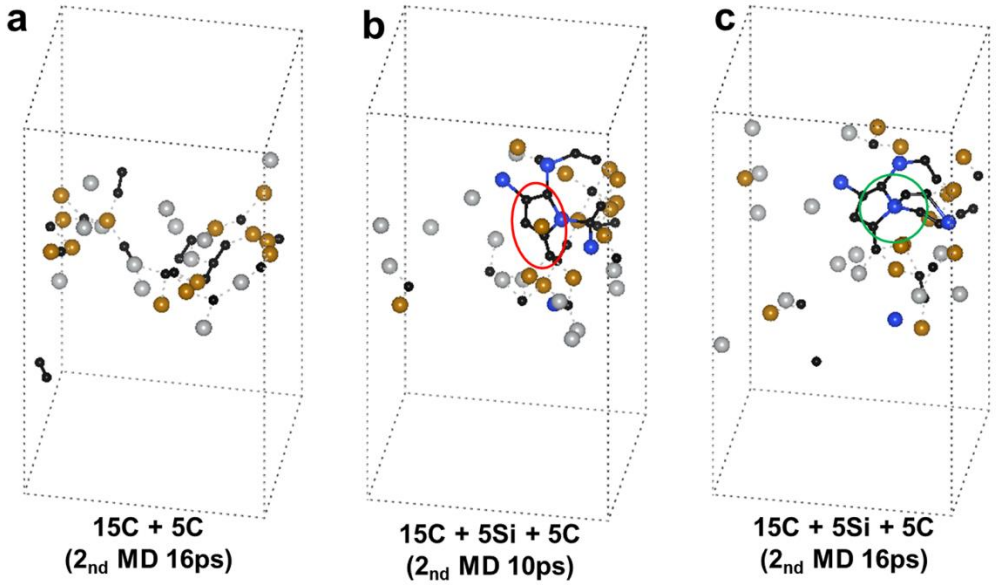

Figure R26. (a) The structure of the solute is shown by excluding the 120 Ga in the slab structure of the Ga-Fe-Ni liquid metal obtained after 18 ps of MD with 15 C atoms and then the 2nd MD of 16 ps by adding 5 more C atoms. There are no carbon clusters larger than C_3. (b-c) Structure in which (b) 10 ps (1st MD of 5 Si and 15 C) and then (c) 16 additional ps in the second MD in which 5 more C atoms were after the 1st MD (of 5 Si and 15 C). The biggest carbon cluster and tetrahedral Si is denoted by red and green circle, respectively.

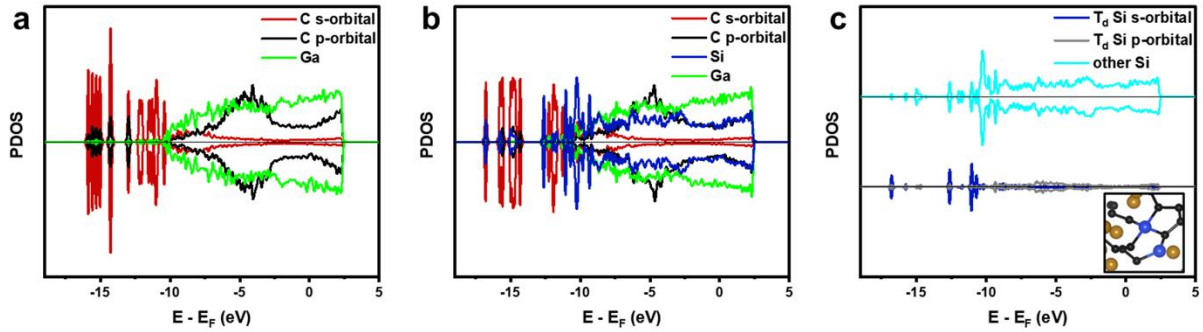

Figure R27. (a) PDOS of the structure shown in Fig. R26a. (b) PDOS of the structure shown in Fig. R26c. The colors used in (a) and (b) are the same as Fig. R24. (c) PDOS of tetrahedral Si surrounded by 4 C atoms (blue and gray indicate Si s- and p-orbital) and PDOS of the other Si (light blue). PDOS is the result of summing each element type and dividing by the number of elements.

In an attempt to test whether Si plays a role in maintaining sp^3-bonding of carbon clusters at some C cluster size, we embedded a diamondoid-like structure (however, with no C-H bonds present) in a pure liquid Ga slab and examined its structural deformation up to 10 ps of 1300 K AIMD. We chose adamantane, $C_{10}H_{16}$, and studied the deformation of the C_{10} core unit with no H's attached, and also a Si_6C_4 cluster in which 6 C's in this C_{10} core unit were replaced with Si; and finally, also clusters in which 1 C atom, or 6 C atoms, were added to Si_6C_4.

Fig. R28 shows each initial and final structure, and the 10 ps MD trajectory is shown in Supplementary Movie 5-8. The C_{10} structure completely lost its sp^3-bonding character and transformed into a chain within 5 ps (Fig. R28a). The Si_6C_4 structure maintained tetrahedral bonding of C to a large extent, i.e., the sp^3-bonding character was maintained relatively well (Fig. R28b). Upon addition of 1 or 6 C atoms to Si_6C_4, it was not deformed into a chain shape (Fig. R28c-d) and tetrahedral bonding persisted. Fig. R29 shows the projected DOS of the initial C_{10}, of the final chain shape C_{10}, and of the Si_6C_4 structure. The C_{10} cluster was thus not stable and indeed has fewer states, with the integration of states in the low energy region shown in gray being 4.03 (Fig. R29a); the C_{10} chain has more states, with the integration of states in the same energy region being 4.98 (Fig. R29b). Chain structures are preferred because they have more states in the lower energy region. In Si_6C_4, a stable cluster structure can be maintained because the integral value of the carbon state in the same energy region was 6.27 (Fig. R29c).

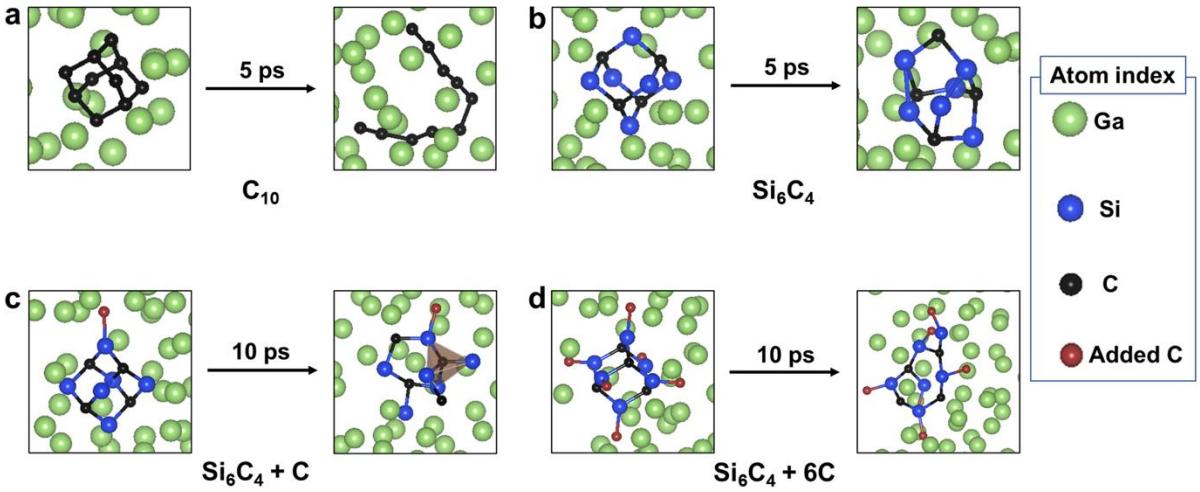

Figure R28. (a) Structure before and after 5 ps MD in liquid Ga of C_{10} structure with all hydrogen removed from adamantane, the smallest diamondoid. (b) 5ps MD results of a structure in which 6 C atoms are replaced with Si in H-free adamantane (thus, Si_6C_4). (c-d) Structures after 10ps, starting from (c) 1 and (d) 6 C atoms were added to the Si_6C_4 structure. In (c) and (d), the added C atoms are shown in brown color.

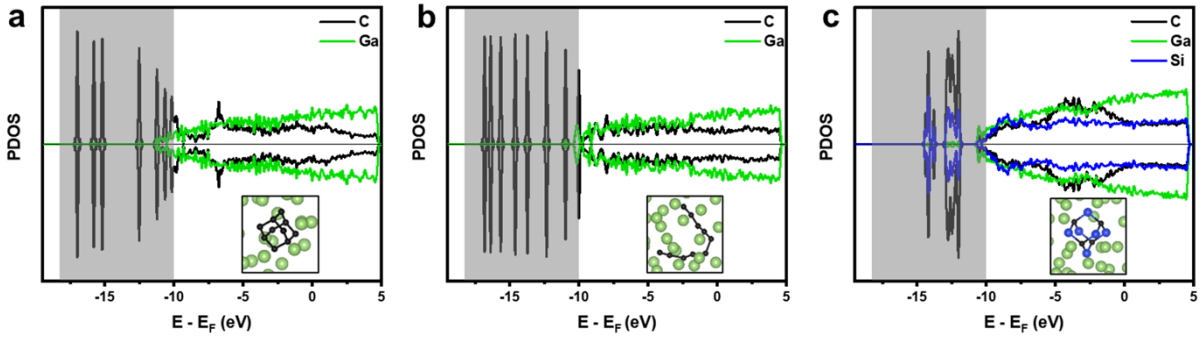

Figure R29. (a-c) PDOS of (a) The C_{10} cluster described in the text, (b) the C_{10} chain that forms, and (c) Si_6C_4. The states of C and Si are shown in black and blue, respectively, and Ga is shown in green.

Our theoretical calculations about the role(s) of Si strongly suggest Si can promote cluster formation (that could be called 'pre-nuclei', as we expect the nucleus to contain (roughly) 20 to 40 C atoms, and one or several Si atoms) with mostly sp^3-like C bonding, in liquid Ga.

Per our modeling at the experimentally relevant temperature of 1300 K, Si has three major roles: 1) C-C bond stabilization, 2) diamond pre-nuclei initialization, and 3) maintenance of sp^3-bonding character. For Si-C-C the calculated formation energy, Bader charges, and projected DOS show that Si makes the C-C bond stable. In the presence of Si, tetrahedral C

can be maintained and a plausible path to diamond nucleation is established in relatively small clusters Si_xC_y. As noted, Si helps maintaining C sp^3-bonding and we find that with Si present, C chains or C chains with Si atoms embedded in such hypothetical chains, *do not form*. But they readily form without Si.

Short summary of theoretical calculations. i) CH_4 is strongly activated when adsorbing on the liquid metal surface per our ability to model that surface-like state, and ii) Si can promote cluster formation ('pre-nuclei') with mostly sp^3-bonded carbon relevant liquid metal models. Our modeling suggests both (i) and (ii) play critical roles in the formation of diamond. And (i) is as mentioned above, strongly supported by experimental studies on pure liquid gallium that show it remarkably activates methane.

2. As the authors stated, Raman spectra of the samples show the presence of diamond together with graphitic carbon. Does this mean graphitic carbon was firstly formed and then was catalyzed into diamond? For example, it has been reported that metal catalysts (or some metal atoms) diffuse into "graphite structure" and catalyze the diamond growth at high temperature, see recent literatures, such as PNAS 119(16): e2201451119 (2022).

Response:

Thank you for your comment.

Our Raman depth-profiling map (Fig. S39) of the as-grown diamond and graphite on the solidified metal piece surface suggests that graphite was *primarily* formed underneath the diamond film (for that film). We note that a *tiny* graphite G band signal was detected when the focal plane was located within the diamond film region, possibly due to the discontinuity of the as-grown diamond film or that *a very small amount of graphite was grown along with diamond*. That graphite was formed primarily underneath diamond (in certain cases, only!) is also suggested by: i) cross-section TEM images showing the graphite structures were underneath diamond crystals with a clear interface (Fig. S38a); ii) EELS spectra acquired from 20 randomly selected regions over the as-grown diamond regions showing only diamond phase

with the absence of graphite phase (Fig. 3e); iii) plan-view TEM images together with SAED patterns of the transferred diamond film showing only diamond phase with the absence of graphite phase (Fig. S25-26); iv) C1s XPS spectrum of an as-transferred continuous diamond film showing only sp^3-bonded carbon without sp^2-bonded carbon (Fig. S28).

For those cases where graphite was found underneath diamond, it suggests that diamonds grow first in the C-rich subsurface region of the LM, followed by the growth of graphite. And we note that graphite was not always formed underneath the as-grown diamonds; for example, there are regions that the as-grown diamonds directly contact the solidified liquid metal surface (Fig. 3a).

In the article (*PNAS* 119, e2201451119 (2022)) mentioned by the reviewer, the authors reported the phase transformation of graphite to diamond catalyzed by Ta during hot-filament CVD under a low pressure (~1600 Pa). The (200) plane of graphite was found to be aligned with the (110) plane of the diamond at the graphite/diamond interface regions. We note that such a kind of 'epitaxy' was also reported in other studies about graphite-to-diamond and diamond-to-graphite transformations. For example, in a recent study with high-resolution STEM characterization of the products from graphite treated under static HPHT conditions, the authors found that the graphite-to-diamond transformation is governed by the formation of nanoscale coherent interfaces, and that graphite domains were intimately connected to diamond domains (*Nature* 607, 486 (2022)). In another study with aberration-corrected TEM characterization on the diamond/graphite interfaces in diamond-to-graphite transformation formed by Ni-mediated transformation of (microwave plasma enhanced CVD) diamond crystals, it was found that the graphitic (0001) planes were connected to the $(\bar{1}1\bar{1})$ surface of diamond (*ACS Nano* 13, 4621 (2019)). Thus, it seems possible and even likely that certain kind(s) of epitaxy should be found at graphite/diamond interfaces when diamond (graphite) is transformed to graphite (diamond).

However, our cross-section TEM image (Fig. R30) suggests that while there is a clean interface between the as-grown diamond film and the as-grown graphite, high-resolution imaging at such interfaces shows no evidence of such epitaxy between diamond and graphite lattices and the absence of bonding between diamond and graphite at the interface regions. As

mentioned, in our growths graphite regions (if present) were mainly found underneath the diamond regions; indeed, we have no evidence that diamond is formed by transformation of graphite in our experimental results.

New text discussing the growth of graphite has been added to the revised Supplementary Information.

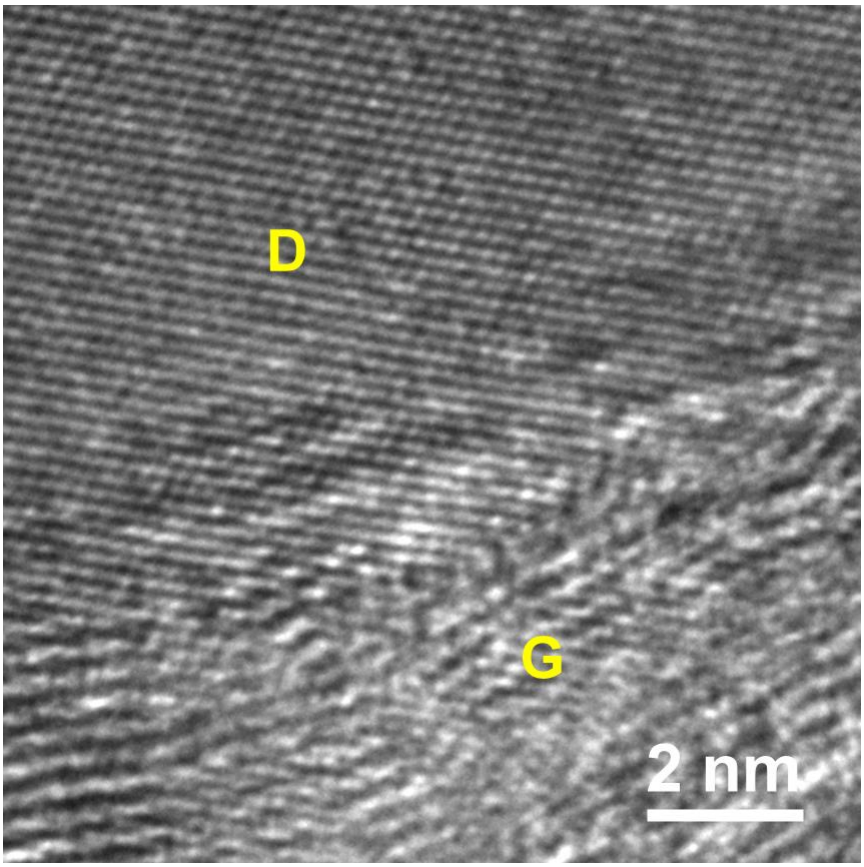

Figure R30. HR-TEM image obtained from the region in Fig. S38a showing the interface between as-grown diamond and as-grown graphitic carbon.

3. Size distributions of the diamond crystals from each typical experiment runs should be statistically counted and compared. Are these Raman bands actually characteristic for nanosized diamonds? (see figure2 and figure S24)

Response:

Thank you for your comment.

We find that for 15 min and 30 min growths, many diamond crystals are partially submerged

having a small portion projecting out of the SLM piece (Fig. R18: 30 min, Fig. 1d: 15 min). We note this strongly suggests that nucleation and growth occurs subsurface. (The reviewer should please note, it is challenging to obtain the *real* size of the many entirely submerged diamond crystals.) To respond to your suggestion of obtaining size distributions we can at this time provide size distributions only of the apex regions that project out of the SLM. But we caution that most of the diamond volume is actually subsurface.

With the above caveat, we studied the sizes of the diamond crystals grown under our optimized growth condition (0.25 at% Si, 11.00 at% Ni, 11.00 at% Fe, 77.75 at% Ga, 1175 °C, 760 Torr, methane/hydrogen 1/20 molar ratio) after growth runs of 15 min, 30 min, 60 min, and 120 min. For each growth run, the size of 200 diamond crystal 'bright regions' were obtained generating the size distributions shown in Fig. R31.

The Raman spectra shown in Fig. 2 and Fig. S37 (that is Fig. S24 in our original submission) *are* typical. We did more Raman maps (50 μm x 50 μm) on the diamonds grown with $^{13}CH_4$ for the configurations (i) liquid metal directly contacting to the crucible bottom surface, versus (ii) placing an EDM-3 Poco graphite plate between the liquid metal and the crucible bottom surface (Fig. 2a) and have added the new Raman maps (Fig. R32) and related descriptions in the revised Supplementary Information.

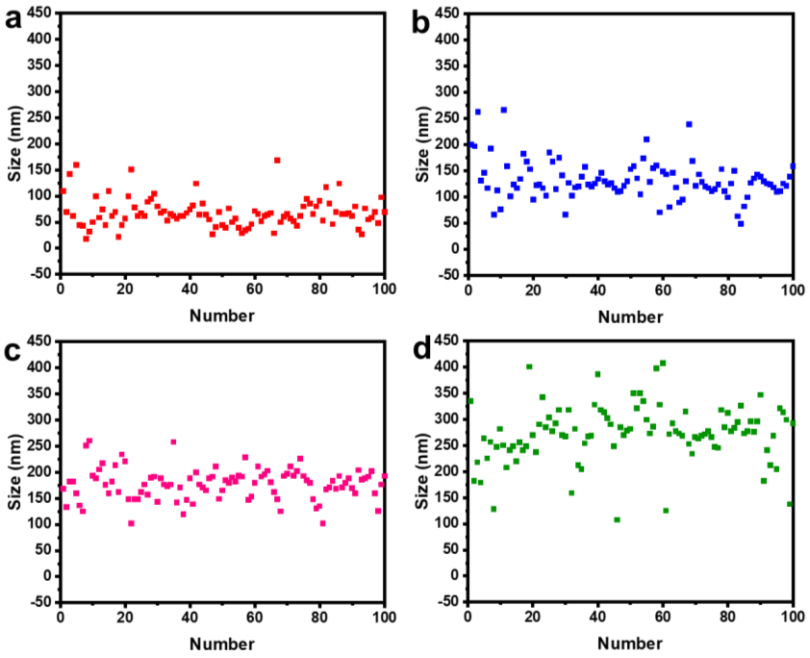

Figure R31. Respective size distributions of the 'bright image' parts of as-grown diamonds that 'project out' of the SLM surface (a) 15 min. (b) 30 min. (c) 60 min. (d) 150 min.

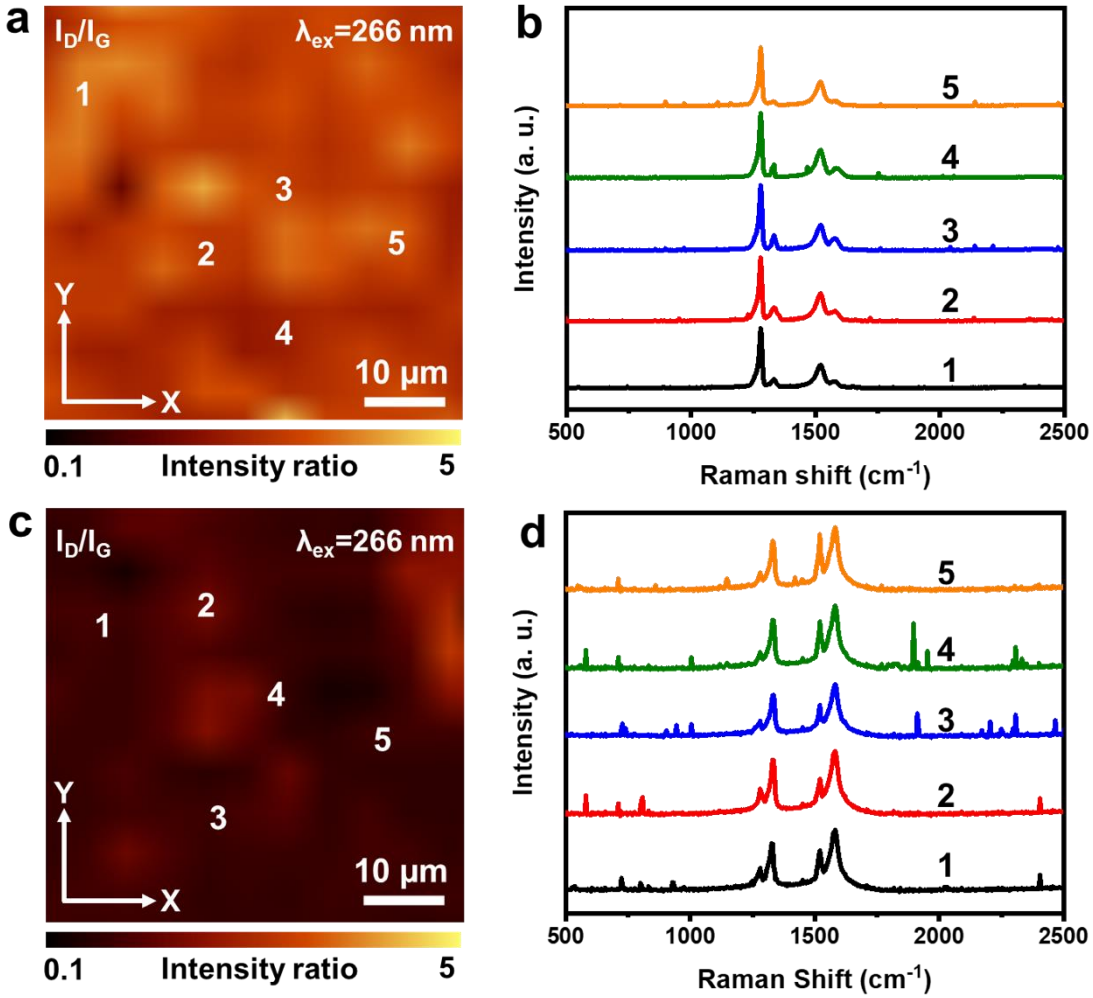

Figure R32. UV Raman analysis of the ^{13}C-D150-EDM and ^{13}C-D150-GC. (a) The Raman map of I_D/I_G ratio of the region in ^{13}C-D150-EDM. (b) Raman spectra taken from the regions marked in (a). (c) The Raman map of I_D/I_G ratio of the region in ^{13}C-D150-GC. (d) Raman spectra taken from the regions marked in (c).

4. It is stated that Si is critical for the growth of diamonds. Did the authors see where the Si went to after the diamond growth?

Response:

Thank you for your comment.

(We also note our remarks about the role of Si in the growth of diamonds in response to your first comment.) Briefly, Si seems likely to participate in (i) stabilizing the formation of small

clusters that can lead to nucleation of diamond in liquid metal (by stabilizing tetravalently bonded carbon or sp^3-bonded carbon—per our DFT calculations). As mentioned, SiV^- color centers are found in our as-grown diamonds. Additionally, a XPS spectrum of the backside of a transferred diamond film shows the presence of trace amounts of Si, with evidence of 'organic silicon' and Si-O bonds found from peak deconvolution (Fig. R4).

We further studied the distribution of Si in the subsurface regions of the solidified liquid metal (optimized condition, after growth of diamonds for 150 min) by using ToF-SIMS depth-profiling (Fig. R33). The regions underneath the as-grown diamonds, and the regions without diamond formed at the surface, were both studied. We note that there are certain amounts of Si found in both regions, and the concentration of Si decreases with increasing depth and reaches constant intensity (ion counts of ~350) when the depth is about 100 nm.

In summary, the Si "went" to 3 regions: i) formation of SiV^- color centers in the as-grown diamonds; ii) trace amounts of Si on the backside surface of the as-grown diamonds; iii) the majority of Si was located in the solidified liquid metal bulk.

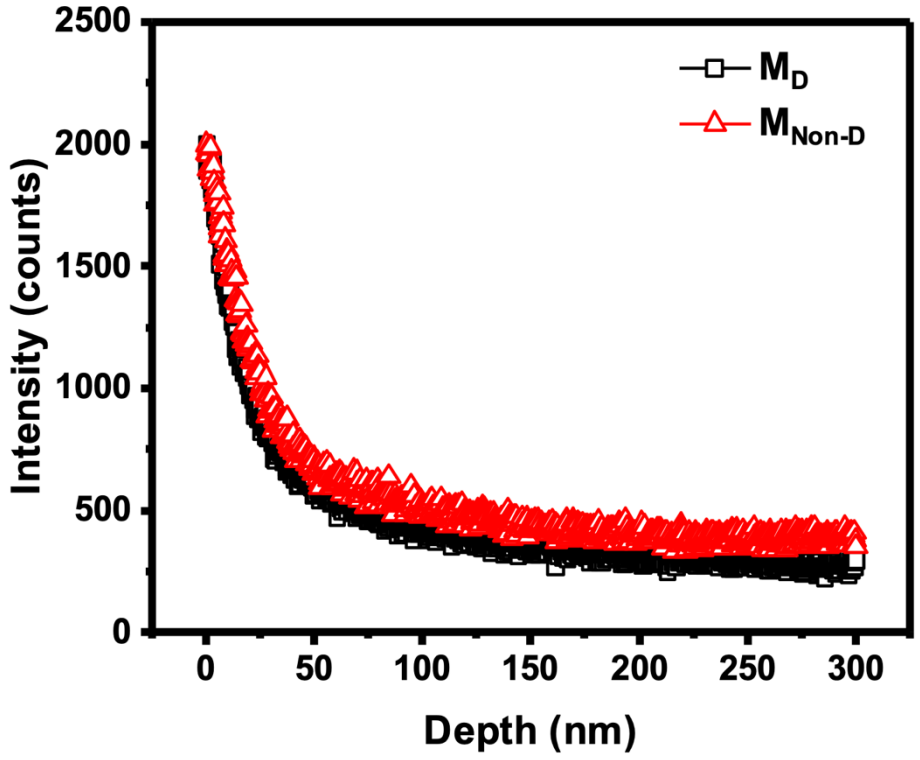

Figure R33. ToF SIMS depth-profiling of silicon concentrations (ion counts as function of the depth from the surface) obtained on two different regions of the solidified liquid metal

pieces.

5. It is very strange that the graphite crucible after annealing shows a much more intense D band than that of the as-received one. Are there any structural changes or reaction due to impurities? Note that the graphite crucible also supply carbon source for the diamond growth. This may affect the diamond formation and should be carefully explored and explained.

Response:

Thank you for your comment.

Please note the 2nd section in the RESPONSES ON TWO TOPICS TO ALL REVIEWERS on pages R4-R5 and thus our *current emphasis* on the use of the EDM-3 graphite piece and the growth of diamonds from methane.

As we stated in our Methods part, our annealing of the graphite crucible (1100 ºC, Ar/H_2 100 sccm / 5 sccm, 760 Torr, 8 h) is done to remove any metallic impurities inside the crucible (even though the company providing the crucibles states that there are none, we have chosen to implement this additional step in our process). We found that the graphite crucible after annealing shows a D to G band intensity ratio about 2x larger than of the as-received one. Such an increase of D band might be due to metal-impurity-mediated H_2 etching of the graphitic structures (*Carbon* 12, 453 (1974); *Journal of Catalysis* 66, 451 (1980); *Nature Communications* 4, 1379 (2013); *Carbon* 96, 311 (2016)). More importantly, we did not find evidence for any diamonds in either the as-received or the annealed graphite crucible by using UV Raman spectroscopy and studying all relevant surfaces.

As mentioned above, the EDM-3 plate does not contribute carbon to the diamond growth. The diamonds grown from the methane are higher quality. **We have thus chosen to focus on always using the EDM-3 plate between the crucible graphite and the liquid metal.**

Certainly, understanding about the mechanism of diamond growth from graphite crucible carbon could be explored in the future either by us or others who read our paper.

6. Is the laser of the pyrometer always on during diamond growth? This may also contribute to

the diamond synthesis (for example, CH4 decomposition).

Response:

Thank you for asking.

The laser light was only used during the set-up of the position of the pyrometer and the position of the graphite crucible. It was not on during growth.

Referee #3 (Remarks to the Author):

The manuscript by Gong et al., entitled “Growth of diamond in liquid metal at 1 atmosphere pressure” presents a novel method for growing polycrystalline diamond films using liquid metal at 1 atmospheric pressure and moderate temperatures (1175°C), in the presence of CH4 and H2 gases. The authors assert that polycrystalline diamond films can be successfully grown at the bottom of a graphite crucible in contact with a liquid metal composed of gallium, iron, nickel, and silicon. They propose that diamond growth is facilitated by the catalytic reaction of liquid metals with carbon sources from CH4. The authors employ various characterization techniques such as HR-TEM, EELS, EDS, XPS, and Raman spectroscopy to confirm the phase-pure nature of the diamonds, albeit with Si-V centers.

This manuscript presents a significant breakthrough in diamond growth, challenging prior assumptions regarding the need for high pressures and temperatures in a liquid phase where diamond is the stable phase. The experimental results are convincing and well-documented. However, reviewer feel that few points addressed below need to be addressed before publication.

Response:

Thank you for reviewing our paper.

1. Comparative Study without Liquid Metal:

Given the similarity in growth conditions between this approach and the hot filament chemical vapor deposition (CVD) process, it is crucial to conduct experiments without liquid metal to

confirm whether diamond growth occurs solely due to the CH_4 and H_2 gas mixture and the elevated temperature. This would provide valuable insights into the necessity of liquid metal in the process.

Response:

Thank you for your comment. We have heated an empty graphite crucible to 1175 ºC (the temperature of the crucible wall reading by pyrometer) under 760 Torr of methane/hydrogen at a molar ratio of 1/20 for 150 min. Our SEM and Raman studies of the crucible bottom surface show that there no diamonds grown (Fig. R34; We note that we extensively explored many regions of the crucible bottom surface by both SEM and Raman.)

Thus, the liquid metal use is critical for the growth of diamonds.

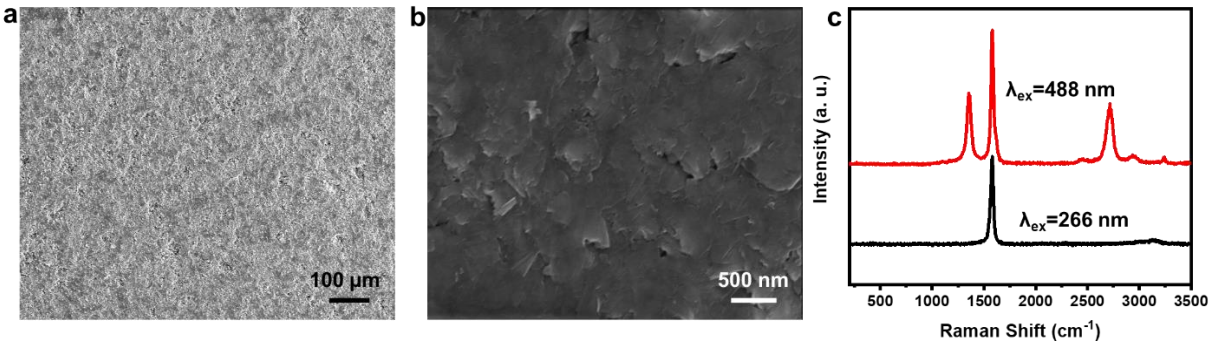

Figure R34. The experiment without liquid metal. (a) The low magnification SEM image and (b) the high magnification SEM image of graphite crucible after running experiment. (c) The Raman spectra obtained by 266 nm and 488 nm.

2. Lack of Theoretical Support:

The manuscript lacks theoretical simulations to support the proposed diamond growth mechanism, particularly diffusion of carbon species at the liquid metal-surface interface. While the experimental evidence is clear, theoretical simulations would add depth to the understanding of the process and help establish a more robust mechanism. However, it is understood that this is not trivial and would need more time/work and it may delay this important result, so this is optional.

Response:

Thank you for your comment.

We have done extensive theoretical modeling that shows: i) a remarkable activation of methane by our models that we could employ of the surface of the liquid metal, ii) a role of Si in stabilizing two carbon atoms (Si-C-C, and C-Si-C), and also in stabilizing tetravalently bonded C, that is, sp^3-bonded C clusters in the liquid metal. Please note our response to the Comment 1b from Reviewer 2 on Pages R30-46.

3. Role of Silicon:

The manuscript mentions that no diamond growth was observed in the absence of silicon. This finding raises questions about the precise role of silicon in the diamond growth process, which the manuscript does not adequately address. It is essential to explore the mechanism through which silicon influences diamond nucleation and growth.

Response:

As we mentioned in our submitted manuscript and we politely feel deserves mentioning again, 0.50 at% Si (and 150 min growth) leads to a much higher density growth of diamonds of smaller crystal sizes; and 0.25 at% Si used for our typical growth yields the diamonds of largest crystal sizes at 150 min growth. And, when no Si is added to the liquid metal, no diamonds grow (Fig. S5). These observations suggest that Si plays a role in the nucleation of diamond.

These experimental results are supported by theoretical simulation about the roles of Si (please see our response to Comment 1b of Reviewer 2 on Pages R37-46). Briefly, our theoretical calculations suggest Si can promote C cluster formation ('pre-nuclei' for diamond growth) with mostly sp^3-like C bonding, in liquid metal. Per our modeling at the experimentally relevant temperature of 1300 K inside liquid metals, Si has three major roles: 1) C-C bond stabilization, 2) small C clusters with Si present are stabilized with sp^3-like bonding, and 3) stabilizing of sp^3-bonded carbon clusters that contain Si.

In summary, the manuscript presents a groundbreaking result in diamond growth at moderate temperatures and at atmospheric pressure using liquid metal. However, to strengthen the scientific rigor of this work, it is recommended to address the points raised above. Once these issues are resolved, this research could significantly contribute to our understanding of diamond growth processes and have broad applications in material science and industry.

Reviewer Reports on the First Revision:

Referees' comments:

Referee #1 (Remarks to the Author):

In the revision, the authors have responded satisfactorily to all my questions by doing and analyzing a large number of new experiments. I recommend publication of this interesting paper.

Referee #2 (Remarks to the Author):

I have carefully read the response and the revised manuscript. The authors have addressed all my concerns. From scientific point of view, I have no more questions and comments on the revised version now.

Referee #3 (Remarks to the Author):

It seems that similar questions on the theorical understanding of the diamond growth mechanism and the role of Si in diamond growth was raised by other reviewers as well. Author has carried out several new experiments as well as theorical investigations to answer all questions and I am glad to see many of my questions have been answered. The quality of the manuscript is improved substantially. I congratulate authors for this remarkable discovery and happy to recommend this revised version for publication in Nature

Author Rebuttals to First Revision:

Response to Reviewers' Comments

Referee #1 (Remarks to the Author):

In the revision, the authors have responded satisfactorily to all my questions by doing and analyzing a large number of new experiments. I recommend publication of this interesting paper.

Response:

Thank you for reviewing our manuscript.

Referee #2 (Remarks to the Author):

I have carefully read the response and the revised manuscript. The authors have addressed all my concerns. From scientific point of view, I have no more questions and comments on the revised version now.

Response:

Thank you for reviewing our manuscript.

Referee #3 (Remarks to the Author):

It seems that similar questions on the theorical understanding of the diamond growth mechanism and the role of Si in diamond growth was raised by other reviewers as well. Author has carried out several new experiments as well as theorical investigations to answer all questions and I am glad to see many of my questions have been answered. The quality of the manuscript is improved substantially. I congratulate authors for this remarkable discovery and happy to recommend this revised version for publication in Nature.

Response:

Thank you for reviewing our manuscript.